

The background features a decorative graphic consisting of several overlapping circles in various shades of blue. Two thin, light blue lines intersect at the top left and extend diagonally across the page. A large, partially visible circle is located in the bottom right corner.

Understanding, characterization, and development of amorphous solid dispersions for poorly water-soluble drugs

By Ahmed Elkhazab

Examiner: Dr. Cornelus F. van Nostrum
Second Reviewer: Dr. Robbert Jan Kok

Department of Pharmaceutics,
Utrecht Institute for Pharmaceutical Sciences,
Utrecht University, the Netherlands.

Writing Assignment (7.5ECTS)
Drug Innovation Masters Program
June 23rd 2014 – July 25th 2014

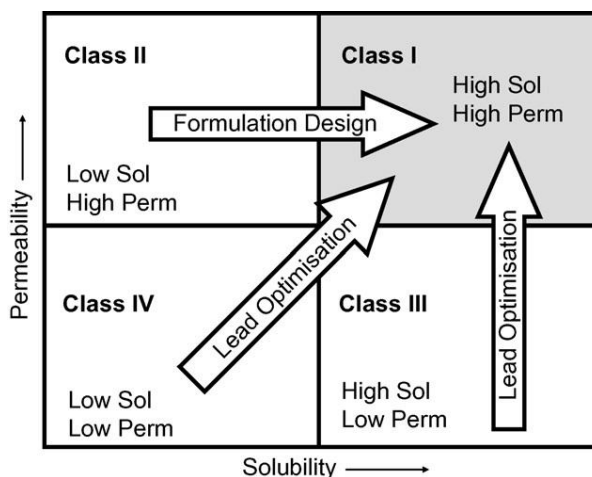
Table of Contents

Table of Contents.....	2
1. Introduction: challenges for oral delivery systems.....	3
2. Definition and description of the amorphous solids against their crystalline counterparts.....	4
3. Factors influencing crystallization.....	6
4. Crystallization process: dynamics overview	9
A. Nucleation.....	9
B. Crystal Growth	11
5. Strategies for inhibiting crystallization	14
A. Inhibition of surface crystallization by nanocoating.....	14
B. Inhibition of crystallization by mesoporous systems.....	14
C. Inhibition of crystallization by API-polymer dispersions	17
6. Influence of manufacturing methods on amorphous solid dispersions	23
7. Summary and conclusion.....	26
8. References	29

1. Introduction: challenges for oral delivery systems

Oral delivery is the simplest way of administration where the drug is taken by swallowing through the mouth. It is the most preferable and commonly used route, due to its high patient compliance and much lower cost. However many active pharmaceutical ingredients (APIs) in pharmaceutical industry have poor aqueous solubility, hence suffer from poor bioavailability after oral administration. The two main key factors in bioavailability of any drug are solubility and permeability. The biopharmaceutical classification system¹ classifies the drug substances according to their solubility and permeability parameters into four different categories as defined by the U.S. Food and Drug Administration (FDA)², demonstrated in figure (1).³

Figure (1) Schematic representation of the biopharmaceutical classification system according to the U.S. FDA. As indicated in the diagram, a drug with poor solubility (exists in class II), can be improved by formulation strategies. On the other hand, a drug with poor ability to pass through the lumen membrane (exists in Class III), should be modified on the molecular level.³



In fact, most of the APIs exist in class II, III and IV, where solubility, permeability or both are limited.^{1,4} For hydrophobic drugs which have poor aqueous solubility in class II, different strategies have been implemented to enhance their dissolution rates. Salt formation is main simple approach to improve solubility, however this is only limited to acidic and basic ionizable drugs that can form salts easily.⁵ Another conventional way is to reduce particle size mechanically by micronization (typically to 2-5um) using air-jet mills or ball mills.⁶ However smaller particles though they dissolve faster, they still hold the same solubility equilibrium. In addition, powdered solids generally suffer from poor compressibility and low flow properties.⁷ Nanocrystals technology by tough ball-milling was later developed which can attain crystalline particle size down to 100–200nm.^{8,9} Further processes of spray drying and adding excipients are required to prevent particle agglomeration after disintegration of the dosage form. In addition, co-crystals were found to absorb water anisotropically after storage and form hydrates upon exposure to elevated relative humidity levels.¹⁰ Another possibility is the use of solubility enhancers as surfactants and emulsifying-agents as in lipid-based delivery.^{11–14} Lipid formulations can enhance the solubility of a drug by formulation in a self emulsifying drug delivery system (SEDDS) and self-micro-emulsifying drug delivery systems (SMEDDS), and allowing the drug to be in a dissolved state within a colloidal dispersion. Despite the potential benefit offered by SEDDS and SMEDDS, it is still possible that the lipid formulation gets digested in the lumen, leading to the precipitation and poor absorption of the drug. In addition, poorly water-soluble drugs are hydrophobic but not necessarily lipophilic, and thus

drugs with low log P values (<2) are always not suitable for lipid formulations.¹⁴ Another disadvantage is the general poor tolerability of surfactants in chronic use.

In recent years as enhancing the oral dissolution and bioavailability becomes more challenging for the pharmaceutical industry, formulation of APIs in the form of amorphous solid dispersions has attracted the utmost attention. Despite being a promising strategy, amorphous solids are thermodynamically unstable compared to crystalline forms, and their physical stability is still a major concern. Moreover, their supersaturation in solution must be maintained even post-administration, thus ensuring complete dissolution and subsequently enhanced bioavailability.¹⁵ The aim of this review is to overview amorphous solid dispersions as potential candidates for oral delivery of poorly water-soluble drugs. First, the differences between amorphous and crystalline forms in terms of orientational structure, physical stability and free energy are elaborated. Next, the factors behind re-crystallization of the amorphous forms are explained. Meanwhile, the review will briefly highlight the two steps involved in crystallization process, nucleation and crystal growth. Afterwards, different strategies for inhibiting crystallization are then approached in detail one by one, such as nanocoating, mesoporous systems and API-polymer dispersions. Each will be discussed in regard to their mechanism of crystallization inhibition, reported evidence in the literature, and the influence of the selected manufacturing method on stability and bioavailability. Finally, a brief discussion assessing the overall data is deduced, followed by some future insights and concluding remarks.

2. Definition and description of the amorphous solids against their crystalline counterparts

Crystalline drugs are well-known to exist in a thermodynamically stable state and thus when presented in their crystalline form to the gastrointestinal tract (GIT), their poor water solubility limit their rate of dissolution, hence they are not well absorbed. The highly ordered and symmetrical structure in the crystal lattice accounts for its strong chemical and physical stability. Conversely, amorphous forms lack the three-dimensional long range order or orientational symmetry that exists in crystals. At best, amorphous can have only some short range orders in their atomic arrangement. Consequently, amorphous forms have greater free energy and molecular mobility in comparison to crystals.

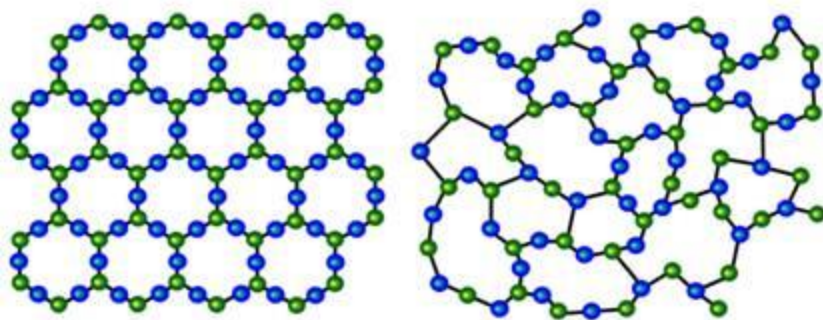


Figure (2) Schematic representation illustrating the difference between of symmetrical lattice structure of crystalline (left) and glassy amorphous lacking long range order (right).

Hancock and Zografi explained the model of enthalpy or specific volume with relation to temperature in the amorphous glassy state, as demonstrated in figure (3).¹⁶ In the crystalline state, a minimal increase in enthalpy and volume is observed in accordance to increasing the temperature, until the melting temperature (T_m) is reached where there is a first-order phase transition to the liquid state. When the process is reversed and the temperature is reduced below the melting temperature (which can be also regarded as freezing temperature), molecular motions starts to slow down significantly. This temperature reduction or supercooling, has to be quick enough to avert crystallization.¹⁶⁻¹⁸ Both enthalpy or specific volume will follow an equilibrium line till a solidification point is reached, afterwards the liquid would exist in a supercooled state. During the transition process, the quick reduction of temperature is accompanied by an increase in viscosity, where the molecules will move very slowly, and thus cannot reorient before the temperature is lowered again.^{16,17,19} Further cooling to a certain temperature would result in a change in the temperature dependence of the enthalpy and volume. This specific temperature is known as the glass transition temperature (T_g), where a change in the slope is usually noticed. Glass-transition is a laboratory phenomenon in which an amorphous solid would undergo a reversible change from a supercooled liquid to a non-crystalline solid-state like, also known as vitrification process.^{17,19,20} This non-crystalline state is referred to as glass. Below T_g , the unstable glassy material exists in a non-equilibrium state where the values of enthalpy and specific volume are higher than the supercooled liquid.^{16,17,19,20} Accordingly, thermodynamic and physical properties of the glassy amorphous solids differ from those of the corresponding supercooled liquid that exist above T_g .

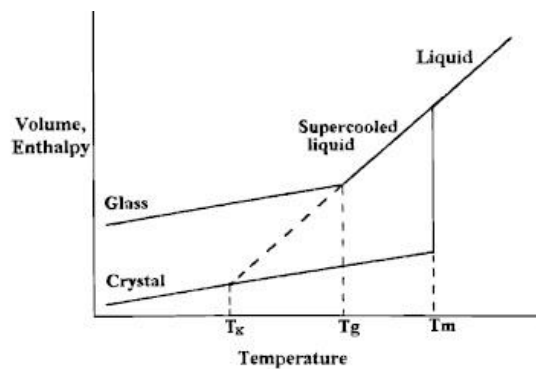


Figure (3) Schematic representation of the specific volume or enthalpy as a function of temperature,¹⁶ illustrating the supercooling of a liquid that can crystallize at T_m , or bypass the crystallization process to a supercooled liquid. Further temperature reduction will lead to the formation of unstable non-crystalline glass at T_g .

Generally speaking, the high internal energy in the amorphous state results in enhancement of the thermodynamic properties of i.e. supersaturation. This leads to better solubility, higher dissolution rates, and subsequently greater bioavailability. Since T_g is the temperature at which the transition state occurs, naturally it would be always lower than T_m . The cooling rate affects T_g , but not significantly (an order of magnitude change in cooling rate, modify T_g by 3-5°C).^{19,20} This is due to the fact that a slower cooling rate will allow more time for the sample to stay available for configurational arrangements and reorientations until the temperature lowers again, thus T_g slightly decreases with lowering the cooling rate.^{19,20,23} When in fact, the cooling rate itself was found to strongly influence other parameters as the rate at which recrystallization might occur and the type of crystal formed, which will be addressed in more detail later in this review. Overall to say, the glass transition exists over a range of temperature, whereas the greater the heterogeneity of the system, the wider will be this transition range.²²⁻²⁴ Further below T_g , exist a critical temperature known as Kauzmann temperature (T_k) as shown in figure (3). At this temperature, the difference in entropies between the liquid and the solid phase becomes zero.¹⁹ Hypothetically with extrapolation, further cooling applied to the supercooled liquid below its T_k ,

suggests that it would have lower entropy than its crystal phase. This controversy is referred to as Kauzmann's Paradox,²⁵ disagrees with Planck's statement of the third law of thermodynamics, as entropy of a liquid would never be less than the entropy of a glass (or solid) of the same enthalpy. Recent evidence from simulations studies of model glasses has confirmed that T_k by its classical definition, only exists in theory and cannot be reached regardless of how the liquid entropy extrapolates, and therefore there is no violation of the third law.²⁶ Therefore T_k can be regarded as an indicative parameter, that would mark the lowest boundary of T_g and estimate how far a liquid can be supercooled before the glass transition must intervene, as $T_g \geq T_k$.¹⁹

3. Factors influencing crystallization

It is well recognized that chemical reactivity is more facilitated as the system shows a higher degree of disorder, and less restricted molecular motion. Consequently, the presence of a material in the amorphous form makes it very liable to spontaneous recrystallization again. The two main instigating factors in the process of crystallization are temperature and relative humidity (RH). Any amorphous form can fully or partially crystallize during different processes of manufacturing, storage and handling. The lower the storage temperature relative to T_g , the lower molecular mobility and more stable the system, therefore crystallization is likely to happen above T_g . However, studies have shown that crystallization can even occur at temperatures well below T_g .²⁷ As shown in figure (4), amorphous indomethacin exhibited crystallization below its T_g at a 30°C temperature range in matter of few days.

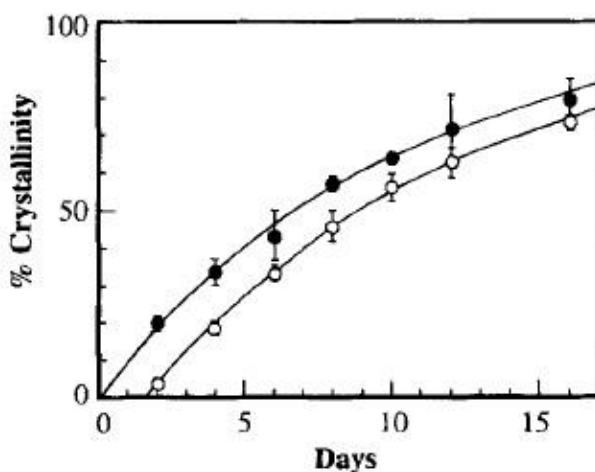


Figure (4) Crystallization of amorphous indomethacin formed by rapid cooling (open circles) and by slow cooling (closed circles) stored at 30°C under dry conditions (T_g of indomethacin is 42°C) as reported by Yoshioka et al.²⁷

These results suggested that amorphous forms prepared in different methods, could display different rates and mechanisms of crystallization, and affect the type of polymorph formed. Above T_g of indomethacin, it was shown that the rapidly cooled amorphous form resulted in the formation of the metastable α -crystal more prevalently, while only the slowly cooled method resulted in the more stable γ -crystal form. Whereas during storage at 30°C (below T_g of pure indomethacin of 42°C), the rapidly cooled amorphous form tended to relax to resemble more the slowly cooled form, subsequently crystallization of both samples below produced the γ -crystal form exclusively.²⁷ Yoshioka et al. explained

the possibility of crystallization below T_g , despite the theoretically much lower molecular mobility and free energy by the dynamics of rotational diffusion. It is assumed that in case of the amorphous state, and even below T_g , rotational diffusion would still be sufficient to allow nucleation between the neighboring molecules, followed by crystal growth. This was supported by the fact that nucleation can occur by rotational diffusion in less than 100 seconds.²⁸

Furthermore, since the two crystal forms are closely related in terms of melting temperatures and heat of fusion, therefore it would be normally assumed that both the α - and γ -forms would appear together even below T_g . This was explained by the investigators by the difference in the interfacial energy at the nucleus-amorphous interface (ΔG_s) between the two crystal forms.²⁷ The more metastable α -form being more highly disordered and having a lower (ΔG_s), will therefore appear first with rapid supercooling, preceding the more stable form, and thus consenting with Ostwald step rule²⁹ for crystallization and solid state transitions. The same can be said for lower molecular mobility and less disorder below T_g , and therefore thermodynamically restricting either the rapidly cooled or the slowly cooled methods towards the formation of the more stable γ -crystals. Later on, when the rapidly cooled sample relaxes to a more ordered state, and the interfacial energy increase, the γ -form would eventually predominate.

On the other hand, amorphous products are typically more hygroscopic, and more water content can be taken up relative to the crystalline form.^{30,31} Unlike adsorption in crystalline solid, which depends on the available surface area for crystal hydrates formation, water uptake in amorphous solids is more related to the total mass available. In amorphous solids, water acts as a plasticizer by minimizing molecular hydrogen bonding and expanding the free volume of the solid. This leads to a depreciation in T_g below the storage temperature, and thereby increasing the risk of chemical degradation and expediting the process of crystallization.³¹⁻³⁵ This plasticization effect can be observed even with small water amounts and it is correlated to viscosity of the solid. And therefore, shifting above the T_g -border depicted in figure (5), the molecular mobility would greatly increase, and the nature of the amorphous material will somehow change to a less viscous rubbery state; where crystallization would be very much favored.³¹ Another illustration of the effect of water content on T_g is presented in table (1), from data by Slade and Levine³² for amorphous sucrose at moisture contents of 0.1% and 0.5%, where T_g of purely anhydrous sucrose is assumed to be 52°C.^{31,32} In addition, presence of excipients is another factor should be taken in consideration.³¹ Water can be brought to the system due to the presence of excipients by means of adsorption, which can result in chemical degradation or affect the rate of crystallinity. The Gordon-Taylor equations³⁶ provides a predictive explanation for the net T_g resulted from ideal mixing of molecules as sugars, polyvinylpyrrolidone (PVP) or indomethacin with water.

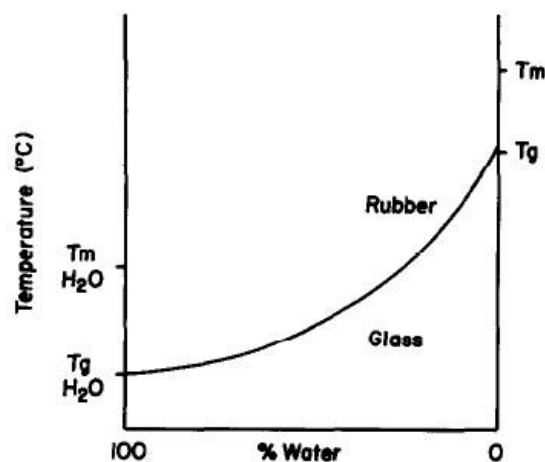


Figure (5) Schematic diagram illustrating water plasticization and its effect on T_g .³¹

$$T_{g_{\text{mix}}} = \frac{w_1 T_{g1} + w_2 T_{g2} K}{w_1 + K w_2} \quad \text{and} \quad K = \frac{\rho_1 T_{g1}}{\rho_2 T_{g2}}$$

Where T_g is the glass transition temperature, w is the weight fractions of the components, and K is calculated from densities ρ of the components and their T_g .

Amount of moisture (%)	Amount of amorphous material (%)	Moisture content in amorphous material (mg H ₂ O/100 mg solid)	Glass transition temperature ^a (°C)
0.1	0.5	20	9
	1	10	27
	2.5	4	45
	5	2	49
0.5	0.5	100	-73
	1	50	-36
	2.5	20	9
	5	10	27

Table (1) Effect of moisture content of 0.1% and 0.5% on T_g of amorphous sucrose by Slade and Levine in 1988, and collected and presented later by Ahlneck and Zografis in 1990.³¹

Andronis et al. studied the crystallization of amorphous indomethacin at different water contents and showed that it can occur at storage temperature at 30°C, below its T_g of 42°C.³⁵ With increasing RH, crystallization rate increases due to an increase in molecular mobility. Another observation was the formation of the stable γ -crystal form below 43% RH, while above 43% RH the metastable α -crystal was the dominant form as demonstrated in figure (6). Earlier, Imaizumi et al. reported, the formation of the γ -form at 79% RH, a mixture of both γ - and α -forms at 89% RH, and only at 100% RH the α -form appeared exclusively, also for amorphous indomethacin held at 30°C.³⁴ To sum up, the physical and chemical stability of amorphous solids relies mainly on the temperature and moisture content. With water behaving as a plasticizer, it is crucial to understand its critical influence on T_g of the system, and relate it to the overall viscoelasticity and molecular mobility of the amorphous form, either in its glassy or rubber phases.

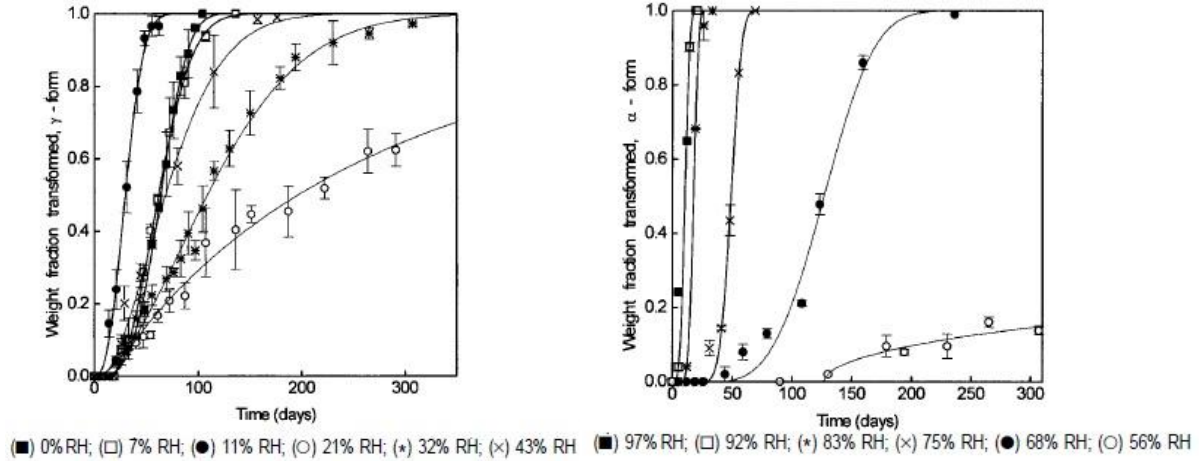


Figure (6) Effect of different % of RH on the crystallization of amorphous indomethacin at fixed storage of 30°C as reported by Andronis et al.³⁵ The γ -crystalline form was formed at lower RH content (left), while the α -form was formed more predominantly at higher RH content (right).

4. Crystallization process: dynamics overview

A. Nucleation

Nucleation is the initial step in crystallization, where a specific arrangement of molecules takes place forming the budding at which additional molecules will accumulate as the crystal grows. Nucleation can either take place in a system which did not have any crystalline matter in the first place (primary) or in the presence of an already crystallized neighborhood in a supersaturated system (secondary).³⁷ Primary nucleation can be classified to homogenous, also referred to as spontaneous, and heterogeneous i.e. induced due to foreign particles. Homogenous nucleation is typically explained by the classical nucleation theory.^{37,38} According to the Classical nucleation theory, the overall free energy of formation (ΔG) for a nucleus of radius (r) is the sum of surface excess energy (ΔG_s) and volume excess energy (ΔG_v) and can be expressed by the two equations:

$$\Delta G = \Delta G_s + \Delta G_v$$

$$\text{and therefore, } \Delta G = 4 \pi r^2 \gamma + \frac{4}{3} \pi r^3 \Delta G_u$$

Where (ΔG_u) is the free energy change, and γ is the interfacial tension per unit area, between phases of crystal and liquid. (ΔG_s) represents an interfacial term concerned with the surface and always denotes a positive value, while (ΔG_v) is bulk term concerned with energy change in regard to volume and is always negative. This is clearly demonstrated in figure (7). The later negative (ΔG_v) must compensate for the positive cost of surface free energy, and once the overall net (ΔG) becomes

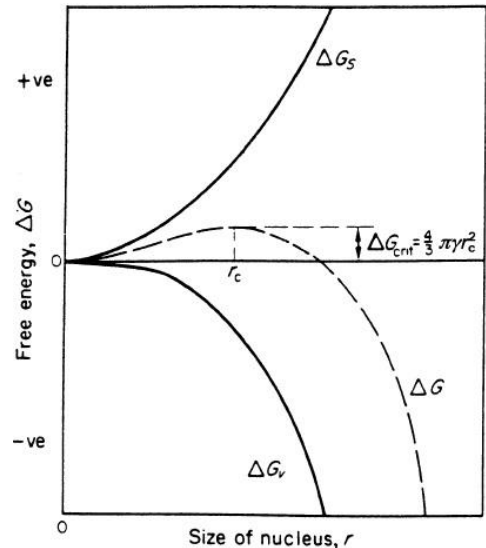


Figure (7) Schematic diagram of the free energy (ΔG) for a nucleus with radius (r).³⁷

negative, nucleation is initiated. At the maximum value of total free energy designated as critical total free energy ($\Delta G_{v_{crit}}$), and hence nucleus of critical radius (r_{crit}), we get:³⁷

$$\text{Where } r_{crit} = \frac{-2\gamma}{\Delta G_u} \quad \text{therefore } (\Delta G_{crit}) = \frac{16\pi\gamma^3}{3(\Delta G_u)^2}$$

Crystalline nucleus initiated in this pattern can have two fates, either grow or redissolve, which depends on the free energy of the nucleus, which in turn depends on the radius. If r is greater than r_{crit} , the nucleus will therefore be stable and continue to grow, and if r is of a lesser size, then the nucleus is most likely to redissolve. Furthermore, the rate of nucleation (J) itself can be expressed by a modified-Arrhenius reaction velocity equation³⁹ for a thermally activated process:^{37,40}

$$J = A \exp\left(-\frac{16\pi\gamma^3 v^2}{3K^3 T^3 (\ln S)^2}\right)$$

Where A is the frequency factor independent from the temperature, v is the molecular volume, K is Boltzman's constant (gas constant divided by Avogadro's number), T is the temperature, and S is the degree of supersaturation. Therefore it is obvious that the nucleation rate is primarily dependant on the interfacial tension, temperature and degree of supersaturation. Increase in the degree of supersaturation and temperature would cause rapid acceleration in the rate of nucleation. The free energy difference (ΔG_u) between the crystalline and the glass phases, in case of supercooling a solid melt can be predicted by Hoffman equation:^{37,40,41}

$$\Delta G_u = \frac{\Delta H_f + \Delta T}{T_m} \quad \text{where } (\Delta T) = T_m - T$$

Where (ΔH_f) is the enthalpy of fusion, (T_m) is melting temperature and (ΔT) is the change in temperature or simply, the supercooling in this case and (ΔT) = $T_m - T$. On substitution in the previous rate of nucleation equation, the following formula is deduced:^{37,40}

$$\text{Given that the critical radius } r_{crit} = \frac{2\gamma T_m}{\Delta H_f \Delta T} \quad \text{therefore } J = A \exp\left(\frac{16\pi\gamma^3}{3K T_m \Delta H_f^2 T_r \Delta T_r^2}\right)$$

(T_r) is the reduced temperature ratio given that $T_r = T/T_m$, or $\Delta T_r = \Delta T/T_m$. From the previous equation we can relate the supercooling to the rate of nucleation. As the supercooling increases, the critical radius will be reduced, and hence less free energy needed to initiate nucleation, and for this nucleus to continue growing.

Likewise, the presence of impurities or foreign elements can affect the nucleation in either a promoting or adversely behavior, and is referred to as heterogeneous nucleation. This is inclusive to atmospheric dust and vapors, as they would be also regarded as hetero- or foreign particles. With the presence of such particles, nucleation can be initiated at a lower degree of supercooling and less free energy that was would be needed for homogenous nucleation of the same glass. Therefore the new less free energy (ΔG)* = $\phi (\Delta G)$, where ϕ is a factor less than 1. ϕ can be calculated by:³⁷

$$\phi = \frac{(1 - \cos\theta)(2 + \cos\theta)^2}{4}$$

$$\text{where } \cos\theta = \frac{\gamma_{sl} - \gamma_{cs}}{\gamma_{cl}}$$

θ is the angle of contact by the foreign object, between both the solid and the liquid phases, as demonstrated in figure (8). (γ_{sl}), (γ_{cs}) and (γ_{cl}) are interfacial tensions between the crystalline solid and the supercooled liquid, the crystalline solid and the foreign object, and the supercooled liquid and the foreign object respectively. Arbitrarily if $\theta = 180^\circ$, ϕ will be equal to 1 and therefore $(\Delta G)^*$ would be equal to (ΔG) . Eventually, the angle of contact is the main variable here that would influence the free energy required to initiate a heterogeneous nucleation.³⁷

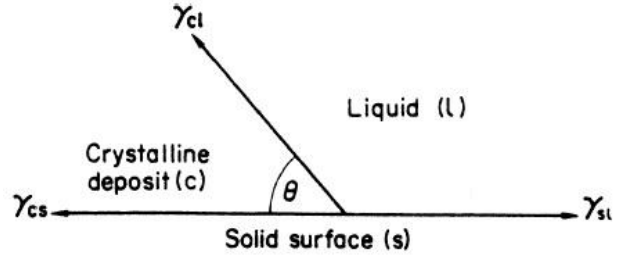


Figure (8) Schematic diagram of the three interfacial tensions at the boundaries of the solid crystalline, supercooled liquid and foreign object.³⁷

B. Crystal Growth

The characterization of the growth of crystals separately from the nucleation process is difficult. The different kinetic model and the lag time between the two events should be taken in consideration.³⁴ The Kolmogorov-Johnson-Mehl-Avrami (KJMA) theory⁴² describes the change in degree of crystal formation as a function of time which relies on the volume fraction of the solid being crystallized:⁴⁰

$$x(t) = 1 - \exp[-K(t - t^*)^n]$$

Where $x(t)$ is the fraction crystallized at time t , K is a constant described by nucleation and growth rate constants, t^* is the induction time and therefore $(t - t^*)$ is the lag time, and n is a constant that describes the growth morphology. The KJMA equations have been widely applied to estimate the overall degree of crystallization and crystal growth in glasses. The Kohlrausch-Williams-Watts equation⁴³ can replace the previous KJMA model to obtain the mean relaxation time at different temperatures:^{40,44}

$$x(t) = 1 - \exp\left[-\left(\frac{t}{\tau}\right)^\beta\right] = \frac{\Delta H_t}{\Delta H_{\max}}$$

Where $x(t)$ is fraction crystallized at time t , τ is the mean relaxation time, β is the constant (equivalent to n in KJMA equation), ΔH_t is the enthalpy at time t , and ΔH_{\max} is the maximum enthalpy that can be recovered, which is equal to the change in heat capacity between liquid and glass:⁴⁴

$$\Delta H_{\max} = \Delta C_p T_g (T_g - T)$$

Where ΔC_p is the change in heat capacity, and T is the storage temperature. This model has been applied in drug-polymer mixtures to estimate enthalpy and heat capacity measurements.^{45,46}

Following nucleation, crystal growth can take place at the surface or in the bulk, as soon as stable nuclei are formed. The crystallization at the surface is generally more feasible, and growth rates are usually more accelerated.⁴⁷ This attributed to several causes. First, the total surface energy required for

nucleation are actually less, where nucleation itself had already commuted area on the surface. In addition, a newly deposited molecule can readily explore the surface to find the best packing, before being buried. Furthermore, the stress usually associated with crystallization is actually more relaxed on the surface rather than in the bulk. Finally, local changes of segregation and oxidation at the surface can often provide a leverage in driving towards crystallization, though not necessarily.⁴⁷ Crystallization at the surface in particular would bring about a crystalline shell, which would adversely affect the absorption and dissolution rates, and hence abolish the pharmaceutical advantage of amorphous formulation.

In organic glasses, crystals can grow faster at the free surface than in the bulk. Wu and Yu investigated the crystallization of indomethacin below of T_g and its underlying kinetics and mechanism.⁴⁸ They found that the crystal growth below T_g (at 40°C) at the free surface was faster than that in the bulk by approximately 100 times. In addition, surface crystallization was proportional to the surface area, however remained unrelated to the sample mass, as shown in the data represented in figure (9). They also reported that the γ - crystal polymorph (more stable), which grows faster than the α -crystal polymorph (less stable), was the more dominant. Interestingly, the initial faster crystallization was followed by a sudden slowdown of crystallization after Indomethacin was partially crystallized, as if a degree of surface crystallization-saturation was achieved at a certain time. Accordingly, they linked the first rapid crystallization to surface crystallization, while the following slower phase to bulk crystallization. A similar bi-phasic crystallization behavior was also noticed earlier for amorphous Phenobarbital by Fukuoka et al.⁴⁹

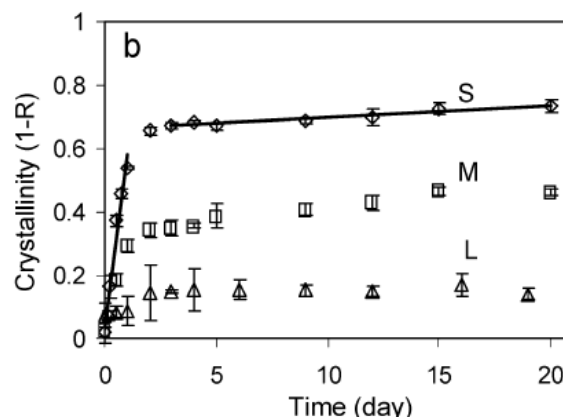


Figure (9) Differential scanning calorimetry readings of amorphous indomethacin powder of different particle sizes, where (S) is small, (M) is medium, and (L) is large, as reported by Wu and Yu.⁴⁸ Smaller particles with greater free surface area demonstrated the higher degree of crystallinity.

Sun et al. investigated the mechanism of crystal growth in indomethacin, and reported that surface crystals have a tendency to rise above the glass surface and grow in a lateral manner, without penetrating deep into the bulk.⁵⁰ Along with high surface molecular mobility, the upward-lateral surface growth increases the surface energy, and thus continuously depositing nanometric layers of crystals on the surface and countervailing the slow growth in the bulk, as shown in figure (10).

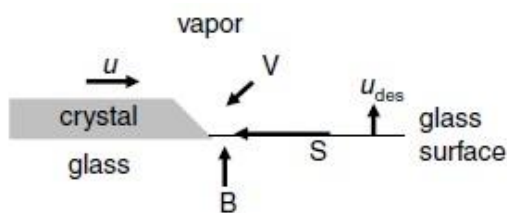


Figure (10) Schematic illustrating surface upward-lateral growth in amorphous indomethacin as reported by Sun et al. Growing crystals rise above the surface and then grow laterally, rather than penetrating into the bulk.⁵⁰

Faster surface crystallization rates by at least one order of magnitude, was also reported for nifedipine below its T_g .⁵¹ Surface crystallization apparently was more promoted below and near T_g , than it was if the sample was held at a temperature significantly above T_g ; an indication that shows that the glassy state itself have a strong tendency for surface crystal growth, and somehow even regardless of the T_g and molecular mobility of the system. Miyazaki et al. supported the claim and showed how factors as structural symmetry and position of functional groups in the molecule can influence the crystallization rate of nifedipine and its analogues.⁵² It is worth mentioning that nifedipine glasses showed even higher rates than indomethacin⁵¹ and felodipine⁴⁴, for both surface and bulk crystallization, despite the fact they all have an approximately equal T_g . The difference in crystallization rate was more pronounced in bulk crystallization rather surface crystallization for nifedipine, and it is believed to be due to its symmetrical structure compared to Indomethacin. According to Zhu et al., this hastened mode of bulk crystal growth in nifedipine is a result of the oscillatory motions associated with supercooled liquid and glasses rather diffusive motions, where the bulk growth is relatively fast for the later to be involved.⁵¹ On the other hand, Felodipine has a analogous molecular structure to nifedipine, and nearly equivalent T_g and molecular mobility, therefore their different crystallization rate cannot be explained by T_g or structural hypothesis.⁴⁴ Investigation showed that higher activation energy for nucleation is observed for felodipine compared to nifedipine, which might be due to stronger hydrogen bonding in amorphous felodipine than in amorphous nifedipine. Interestingly, the case is reversed for the crystalline states for both molecules where hydrogen bonding is stronger in nifedipine than in felodipine, and thus the physical properties of the crystalline counterpart should be taken in account as well as the properties of the amorphous form. Furthermore, on measuring surface self-diffusion coefficients of indomethacin and nifedipine, the later exhibited faster surface diffusion rates and mobility, which indicates substantial surface rearrangement occurring very rapidly.⁵³ It is possible that nifedipine showed higher surface diffusion due to its lower cohesive energy and weak hydrogen bonding compared to indomethacin, attributed to the absence of the carboxylic group in nifedipine, as demonstrated in figure (11).

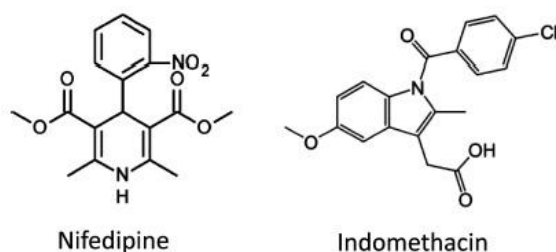


Figure (11) Chemical Structure of nifedipine (left) and indomethacin (right).

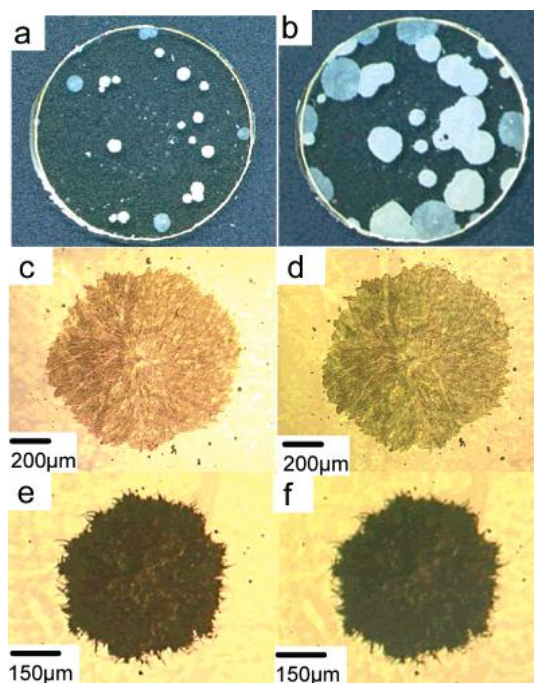
Unlike organic glasses, inorganic glasses do not show faster crystal growth. Diaz-Mora et al. measured the velocities of crystal formation for silicates in the bulk and of the surface in the glass volume, as well as of isolated crystals on the glass surface, and found them to be equal.⁵⁴ The same observation was reported by Wittman and Zanotto for Anorthite glass.⁵⁵ Therefore, mechanisms of interfacial rearrangements that command crystal growth in the surface and bulk are apparently the same in inorganic matter.

5. Strategies for inhibiting crystallization

A. Inhibition of surface crystallization by nanocoating

As discussed before, surface crystallization is a potential threat to the stability of amorphous pharmaceuticals. Besides its role in crystal growth, surface is an attractive environment for heterogeneous nucleation to be launched.^{54,55} Surface crystallization in amorphous forms is commonly attributed to the high molecular mobility and the low viscosity at the surface relative to the bulk. Interestingly, this highly mobile surface was found to be only few nanometers in thickness, and evidence showed that this mobile surface can be immobilized by contact with a solid surface i.e. coating.⁵⁶ A 10 nm coating of gold or polyelectrolyte was sufficient to inhibit the surface crystallization of amorphous indomethacin.⁵⁷ The gold-nanocoating also inhibited the growth of existing crystals, as shown in figure (12). More importantly, the nanocoating with polyelectrolyte did not adversely affect the dissolution rate of the amorphous indomethacin, and enhanced its wetting and flow. The same 10nm layer of gold coating was tested in amorphous nifedipine.⁵¹ As a result the rate of surface crystallization was dropped down to be equivalent to the slow rate of bulk crystallization, where surface crystal growth was already one order of magnitude faster than that of the bulk below T_g for nifedipine, as mentioned before. Eventually, this ultrathin coating technique holds much potential for stabilization of amorphous drug forms, and is yet to be investigated in other amorphous molecules exhibiting fast rates of surface crystallization.

Figure (12) Microscopic images showing the impact of 10nm gold coating on surface crystallization of amorphous indomethacin held at 40°C as reported by Wu et al.⁵⁷ (a) Uncoated indomethacin after 90hours. (b) Same as (a), but 7 days later. From (c) to (f) are nano-coated partially pre-crystallized indomethacin samples, where further crystal growth is inhibited. (c) γ -crystals after 90hours. (d) Same as (c), after 7 days. (e) α -crystals after 90hours. (f) Same as (c), after 7 days.



B. Inhibition of crystallization by mesoporous systems

One of the emerging trends in recent years in the stabilization of amorphous drugs is the addition of mesoporous materials as silicon and silica, in the amorphous formulation.⁵⁸⁻⁶⁰ A porous material is the one having nano-pores or capillaries in its structure, and therefore large surface area (above 500m²/g).⁶¹

Typically, mesoporous materials have an average pore size between 2 and 50nm. Due to their large surface area, a complex process of physisorption takes place by multilayer adsorption and spontaneous capillary condensation.⁶¹ Generally, the adsorption of an amorphous drug on a mesoporous material restricts the system to a lower free energy state (ΔG), hence stabilization of the amorphous form.⁶⁰ A depression in the molecular mobility of amorphous molecules in confinement with adding mesoporous materials is also observed. In addition, these nano-sized pores and capillaries exert locative constraints on the clusters of molecules, thereby obstructing the formation of a nucleus of critical size and preventing crystal growth. This was demonstrated in *o*-terphenyl formulated with controlled pore glass (CPG) materials of diameter ranging between 4 and 73nm.⁶² With decreasing the pore sizes, T_g shifts to a lower temperature. More importantly, at the smallest pore size of 4nm, crystallization of *o*-terphenyl was inhibited completely regardless of the degree of pore-filling. Reasonable explanations were related to the calculations of the critical nucleus of *o*-terphenyl; being larger than the pore size of 4nm, plus the lack of sufficient hydrogen bonding.

Furthermore, various poorly water-soluble drugs were prepared in confinement with mesoporous silicates and their stability and dissolution rates were evaluated *in vitro* and *in vivo*. Ordered mesoporous materials such as MCM-41 and SPA-15 with a periodic arrangement of parallel cylindrical pores with uniform size, were the most widely inspected silicates. Speybroek et al. investigated ten different compounds with poor aq. solubility (carbamazepine, cinnarizine, danazol, diazepam, fenofibrate, griseofulvin, indomethacin, ketoconazole, nifedipine, and phenylbutazone) embedded in hexagonal periodic mesoporous silicate SBA-15.⁶³ All drug/SBA-15 formulations were prepared at a 20% drug loading ratio, and stored at room temperature 25°C and RH of 52% for 6 months. Results demonstrated successful drug encapsulation of average 20% of drug content (highest drug loss was only 1.6% for indomethacin). *In vitro* release results revealed that all drug/SBA-15 formulations were stable for 6 months, and exhibited enhanced dissolution rates with 80% release in 5 minutes versus their crystalline counterparts, as displayed in figure (13), with the exception of danazol. Absorbed fractions were all confirmed to be non-crystalline.

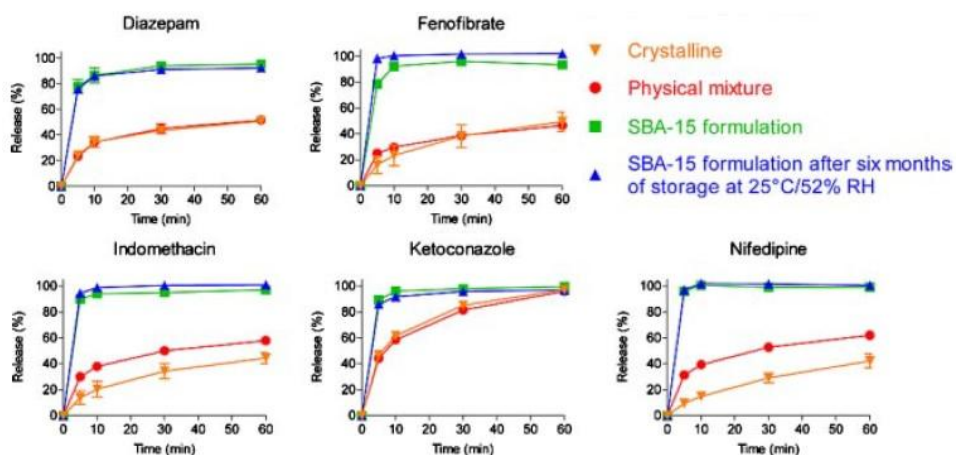


Figure (13) *In vitro* dissolution profiles of five out of the ten drugs embedded in the mesoporous silicate SBA-15 as reported by Speybroek et al.⁶³

In another study, physicochemical stability of indomethacin formulated with ordered mesoporous silica MCM-41 and SBA-15 was studied for 3 months of storage at 30°C and RH of 56%.⁶⁴ Despite overall stability was somehow satisfactory, some chemical degradation of indomethacin was observed in the MCM-41 samples after stressed storage. Still, dissolution rates of both silica formulations were enhanced at a pH range from 1.2 to 6.8 compared to crystalline indomethacin. Moreover, ibuprofen spray dried with SPA-15 remained stable under severe storage conditions of 40°C and RH of 75% for 12 months.⁶⁵ More importantly, a drug loading ratio up to 75:25 (Ibuprofen: SBA-15) was successful, and the dissolution rate was significantly enhanced. Using the same SBA-15, itraconazole were also co-formulated and *in vitro* release was evaluated.⁶⁶ Interestingly, *in vitro* release curves showed that itraconazole dispersed in SBA-15 of pores sizes between 6.4 and 9nm was promptly released; however at pore size of 4.5nm the release was significantly diminished. This suggests a certain critical pore size exist for each drug molecule, below which diffusion and release might be sterically hindered. Similarly in another study, two different types of silica were compared.⁶⁷ Ordered mesoporous silica MCM-41 and non-ordered silica gel Syloid 244 FP EU were both loaded with indomethacin, with excipients and compressed into tables. Neither of the two silica materials showed problems during the tableting process, and both exhibited enhanced dissolution rates. The release rate was a little faster from the non-ordered Syloid 244 FP EU than from the ordered MCM-41, likely to larger pore size and smaller particle size of the former.⁶⁷ Telmisartan, an angiotensin II receptor antagonist, was impregnated with spherical mesocellular foam composed of an interconnected 3D pore system of uniform spherical cells with relatively large size.⁶⁸ These mesocellular foam formulations showed high encapsulation efficiency of 42% and favorable release profile versus both SPA-15 and the crystalline form in both gastric and intestinal simulated fluids. The authors argue that the advanced 3D pore system and the large pore size of the mesocellular foam, permitted easy diffusion and release profiles, while in the 2D hexagonally ordered SBA-15, release might be partially hindered. However more evidence needs to be provided in the future concerning the stability of the mesocellular foam on long term storage and the risk of crystallization.

Due to its promising results, *in vivo* bioavailability assessments were also performed for the ordered mesoporous silica formulations. The oral bioavailability of itraconazole dispersed into SPA-15 and MCM-41 as carriers were evaluated in rabbits and dogs.⁶⁹ In both species, results showed that absorption rates of Itraconazole loaded into silicates was superior to the crystalline form of the drug and comparable with the marketed product Sporanox® (amorphous/HPMC formulation). Furthermore, Itraconazole was loaded onto SPA-15 along with/without precipitation inhibitors, hydroxypropylmethylcellulose (HPMC) and hydroxypropylmethylcellulose acetate succinate (HPMCAS), and absorption was evaluated in rats.⁷⁰ Formulation with HPMC lead to 60% increase in absorption, compared to formulation without HPMC. Additionally, HPMCAS did not enhance absorption, despite being effective in inhibiting itraconazole precipitation, owing to its insolubility in stomach. The aim of adding HPMC and HPMCAS was to extrastabilize the amorphous form, prolong the supersaturation, and further delay the onset of crystallization. The strategy is indeed a novel approach to combine both polymers and silica to prevent crystallization and enhance dissolution and bioavailability.

C. Inhibition of crystallization by API-polymer dispersions

Over the last two decades, the major strategy for formulating stable amorphous solid dispersions was dispersing an API in a polymer. There are many examples of these polymers including trehalose, dextran, polyethylene glycol (PEG), cellulose acetate phthalate (CAP), methylcellulose (MC), hydroxypropyl methylcellulose (HPMC), hydroxypropyl methylcellulose acetate succinate (HPMCAS), and hydroxypropyl methylcellulose phthalate (HPMCP), poly(vinylpyrrolidone) (PVP), poly (1-vinylpyrrolidone) vinyl acetate copolymer (PVP/VA), polyvinyl acetate (PVAc), polyvinyl acetate phthalate (PVAP) and the Eudragit acrylic acid-based polymers.⁷¹ In these API-polymer systems, several important factors must be taken in consideration. Initially, a single-phase amorphous mixture of both the API and the polymer must be obtained, where only one T_g will be observed by differential scanning calorimetry (DSC), and no phase separation is detected by techniques as X-ray diffraction or solid-state nuclear magnetic resonance.⁷¹⁻⁷³ Only the true miscibility of both components would represent a thermodynamically stable single-phase dispersion, capable of displaying favorable dissolution and bioavailability results. Related to the miscibility, is the relative solubility of the API in polymers, which define the maximal API loading that can be achieved without invigorating its tendency for crystallization.^{74,75} Due to the high viscosity of polymers, it is difficult to measure the API solubility in polymers. This difficulty is even more pressing at low temperatures near T_g with low molecular mobility, making it hard to reach the solubility equilibrium. Sun et al. developed a novel method for measuring the API in polymer solubility by annealing the sample at several temperatures to detect the upper and lower bounds of the equilibrium solution temperature, followed by rapid scanning by DSC to detect undissolved crystals.⁷⁵ The method offered a predictive model for detecting the solubility of an API in different polymers, where its significance lies in selecting the most appropriate polymers for formulation, based on solubility criteria. By comparing the solubilities of indomethacin and nifedipine in PVP and PVAc and their co-polymer PVP/VA, PVP displayed the highest solubility capacity for both APIs expressed in %w/w, followed by PVP/VA, and finally PVAc, as shown in figure (14).⁷⁵ Paradoxically, PVP is the most hydrophilic (and hygroscopic) polymer out of the three, yet had the highest dissolving power for both APIs which are considered hydrophobic molecules. To explain this, the authors fitted API-polymer interactions to the Flory-Huggins model:^{75,76}

$$\ln \alpha_1 = \ln V_1 + \left(1 - \frac{1}{x}\right)V_2 + P V_2^2$$

Where α is the API's activity in a saturated solution, V_1 is the volume fraction of the API, V_2 is the volume fraction of the polymer, x is the molar ratio of the polymer and the API (or assumingly the molecular weight ratio), and P is the API-polymer interaction parameter. The API activity decreases with the increase of polymer volume fraction, and this rate depends strongly on the polymer used (molecular weight ratio between polymer and API). On calculating the API-polymer interaction values, PVP had the strongest interaction with both APIs, followed by PVP/VA, and then by PVAc. PVP was previously shown to form strong hydrogen bonding interaction with indomethacin.⁷⁷ In addition, this also explains why indomethacin overall solubility in the three polymers was higher than that of nifedipine, as indomethacin is a good hydrogen bond donor, unlike nifedipine which lacks the carboxylic group as mentioned earlier.

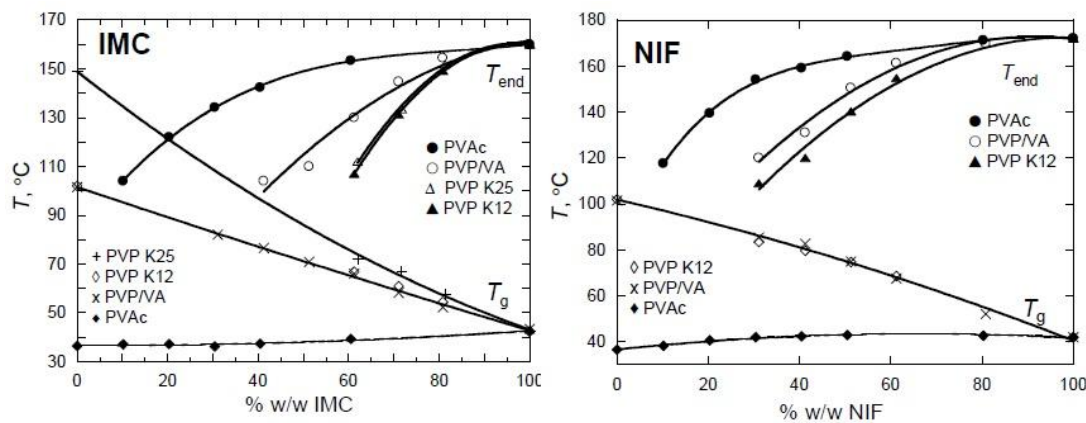


Figure 14 Solubility expressed in %w/w for indomethacin (left) and nifedipine (right) in different polymers of PVP, PVP/VA, or PVAc. For both molecules, dissolving powers were PVP > PVP/VA > PVAc.⁷⁵

Another important factor is the dissolution of these amorphous dispersions in the GIT, even in the presence of high levels of a hydrophobic API. Surfactants, such as Tween 80, Span 80, sodium lauryl sulfate (SLS), D- α -tocopheryl polyethylene glycol 1000 succinate (TPGS), are usually added to facilitate dissolution of the API from the amorphous dispersions.⁷¹ In addition, surfactants can assist in the formation of amorphous dispersions particularly during the hot melt extrusion manufacturing process, as they lower the viscosity of the melt, and consequently increase the overall homogeneity in the API-polymer dispersion.^{71,78} However the physical stability of the amorphous dispersions has been questioned with adding surfactants, whereas surfactants may act as plasticizer, by lowering the T_g and increasing the water uptake in the system, and possibly promoting crystal growth.⁷⁹ Yet again in the presence of polymer, this effect have been shown to be very minimal.^{79,80} Another study demonstrated that the presence of surfactants as Tween 80 and SLS would even promoted dissolution in partially recrystallized indomethacin.⁸¹ Besides the aforementioned factors, a certain degree of supersaturation should be achieved and maintained. In other words, the amorphous dispersions would normally contain higher amounts of API exceeding the normal equilibrium solubility of the API in their crystal forms. Studies have shown that the maximum values of API load in the polymer are generally limited;^{74,75} otherwise the thermodynamic stability of the system would be altered, and crystallization would be favored. These values are commonly low at temperatures near and below the T_g, and therefore supersaturation is necessary in these one-phase dispersions.⁷¹ Furthermore, post-administration supersaturation should also be maintained, even with rapid dissolution of the API and the polymer in the GIT. Polymers as HPMCAS have been demonstrated to be very effective in this case, by inhibiting the possible solution-mediated crystallization of the API (GIT crystallization), and at the same time preserving the API rapid dissolution and high bioavailability.⁸² Accordingly, supersaturation is dependent on the tendency for the API to remain associated with the polymer, even in the GIT. Likewise, surfactants whether added as excipients or naturally existing as bile salts, have been also shown to aid in preventing solution-mediated crystallization by promoting micellization and other colloidal aggregates formation.⁷¹

At storage temperatures, the capability of any polymer to inhibit crystallization and improve dissolution and bioavailability is dependent on several parameters. First, the proportionality of the T_g of the

polymer relative to that of the API, and how far the polymer can raise the overall T_g of the amorphous dispersion. As mentioned before, raising the T_g above the storage temperature will result in lowering the molecular mobility of the system and reduction in the overall free energy, hence limit its tendency to crystallize. In 1995, Hancock et al. introduced a well-known rule of thumb, where the amorphous dispersions should be ideally stored at temperatures that are 50°C or more below the T_g of the dispersion.⁸³ Until nowadays, this rule is still applied in pharmaceutical industry, where the physical stability of the amorphous dispersions was shown to be maintained for long time scales of few years. Moreover, the capacity of molecular interactions between the polymer and the API in the dispersion, through hydrogen bonding, had been shown to be crucial in inhibiting crystallization.^{75,77} Even small amounts of the polymer have been shown to substantially inhibit crystallization in several studies.^{77,83-85} The hydrogen bonding can directly interfere with the nucleation and crystal growth processes, and the degree of crystallization inhibition is proportional to the strength of interaction. There are cases where the significance of T_g and molecular mobility was found to be very minimal. Miyazaki et al. studied the crystallization rates of nifedipine enantiomers with HPMC and HPMCP polymers.⁸⁶ The results showed that the crystallization rate at 60°C of the (+) enantiomer was lower than that of the (-) enantiomer in the presence of any of the two polymers, therefore suggesting that the interaction between the API enantiomers and HPMC or HPMCP is stereo-selective, having in mind that both enantiomers have similar T_g profiles and molecular mobility. Arguably, a recent study by Powell in 2013 revealed that the polymer's strength in inhibiting crystallization is more correlated with polymer's neat T_g , rather than the API-polymer hydrogen bonding interactions.⁸⁵ 1% wt of six polymers; PVP, PVAc, PVP/VA, HPMCAS, polystyrene (PS), and polyethylene oxide (PEO), were doped in nifedipine glass by cryomilling, melting and cooling, and the rate of crystal growth was monitored below and above T_g . The significance of using such a small proportion of the polymers was to limit their influence on raising the overall T_g of the system, which is why the authors referred to the process with the term 'doping' rather than the conventional case of an API being co-formulated or dispersed in a polymer. With the exception of PEO, all polymers resulted in a reduction in bulk crystal growth below and above T_g , as demonstrated in figure (15).

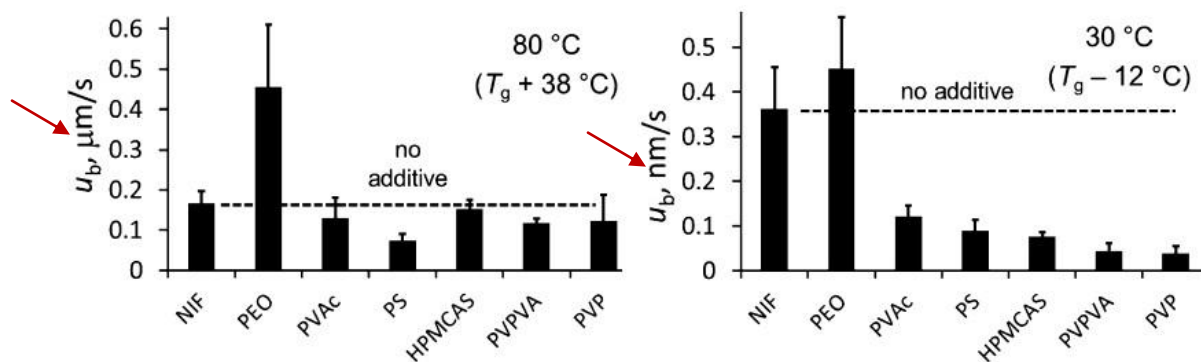


Figure (15) Impact of 1 wt % of six different polymers on nifedipine bulk crystal growth at 38°C above T_g (left) and 12°C below T_g (right), where u_b is the bulk crystal growth rate.⁸⁵

The results suggested that crystal growth inhibition is directly related to the T_g of the neat polymer, where the order of crystal growth inhibition was directly proportional to the T_g of the polymer. In other words, the higher the T_g of the polymer, the more reduction in crystal growth as in PVP case, which had the highest T_g of all used polymers as shown in table (2).⁸⁵ This was further elucidated by Powell et al., by the relation between the T_g of the polymer and the molecular mobility of the polymer's chains. As the T_g of the polymer increases, the segmental mobility of the side chains will decrease. It is therefore suggested that the polymer chains molecules must move out of the way making space for crystals to form, and that with less restricted segmental mobility, the chances of crystal growth or expansion in the bulk are diminished. Remarkably, this hypothesis came in agreement with the classical nucleation theory, where a critical nucleus radius must be reached for nucleation to be initiated as stated before.^{37,38} On the whole, the rate of crystal growth in a API-polymer dispersion below T_g could be linked to both the mobility of the polymer and the overall molecular mobility of the system. Whereas above T_g where the molecular mobility and the free energy of the system are relatively higher, the influence of segmental mobility was seemingly less, and the rate of crystal growth inhibition could be then attributed to other factors as hydrogen bonding interactions.

substance	M_w , kg/mol	T_g (°C)
NIF	0.346	42
PEO 8k	8	-19
PEO 100k	100 (M_v)	-47
PEO 8000k	8000 (M_v)	-53
PVAc 15k	15	30
PVAc 83k	83	36
PS 1.8k	1.78	53
PS 8.4k	8.4	91
PS 17k	16.6	93
HPMCAS-MF	18	114
PVPVA 64	45-70	102
PVP K12	2-3	102
PVP K15	8	120
PVP K30	44-54	164
PVP K90	1000-2000	176

Table (2) Polymers used and their corresponding molecular weights and T_g s, as reported by Powell et al.⁸⁵

But since organic glasses generally exhibits crystal growth more rapidly at the surface than in the bulk, does polymer addition have a similar effect on both modes of crystal growth? A recent work by Ting et al. revealed that PVP displayed a strong crystal growth inhibition in nifedipine at the bulk, but a much weaker impact on crystal growth at the surface.⁸⁷ At 12°C (below T_g), every increase in %wt of PVP by one unity, delayed the crystal growth of nifedipine by 10 times in the bulk, and only 2 times in the surface. The rapid upward-lateral surface crystal growth enabled by the high surface molecular mobility observed in molecules as nifedipine and indomethacin^{50,51} could explain the evasive behavior of surface crystals towards polymer molecules and their side chains, making them less likely to be affected by segmental mobility factors.^{85,87} Another supporting reason was that polymer molecules would theoretically be existing at lower concentration at the surface than in the bulk, as a result of geometrical effects.

Finally in this section, many *in vivo* studies of various amorphous solid dispersions based on API-polymer amorphous dispersions are gathered and surveyed, in order to establish an overview which evaluates their clinical performance and their potential experimental evidence. The assessment of these polymer-based amorphous dispersions in the literature can be categorized into two main directions. The first is the evaluation of the physical stability of the formulation under moderate to severe storage conditions; that is to say monitoring parameters as the formation of crystals, the impact on T_g , and the extent of water uptake. On the other hand, the main criterion in many other papers is assessed based on their *in*

vivo performance in an animal model, or sometimes in human volunteers, and whether they exhibited an enhanced dissolution and oral bioavailability or not. Meanwhile, these parameters are compared with that of a reference entity(s); usually in this case the crystalline form or a marketed product. Some examples of dispersions which contain both polymer and surfactant are also included, considering that the polymer was the main component. In table (3), the collected information is summarized and categorized according to the polymer used in the amorphous dispersion.

Polymer (with/without surfactants)	API (ratio to polymer)	Human/Animal model	Compared against	Bioavailability outcome
CAP	Itraconazole (1:2)	Rats	Sporanox®	2-fold improvement in AUC and bioavailability ⁸⁸
PEG-3350 (with polysorbate 80)	Unnamed drug	Dogs	Micronized drug capsule	15-fold improvement in AUC and bioavailability ⁸⁹
PEG-4000	Esomeprazole zinc	Humans	Nexium® (enteric-coated tablet)	Lower C _{max} but longer T _{max} with almost similar AUC ⁹⁰
			Crystalline form of lonidamine	1.5-fold increase in AUC ⁹¹
	Lonidamine	Rats	Cyclodextrin formulation	Slightly decrease in AUC ⁹¹
PEG-4000 (with/without Phosphatidyl-choline (PC))	Nifedipine	Rats	With vs. without PC	3.4-fold improvement in bioavailability ⁹²
PEG-6000	Nifedipine	Rabbits	Crystalline form of nifedipine	6-fold improvement in bioavailability ⁹³
			SLS formulation	3.6-fold improvement in bioavailability ⁹³
			Cyclodextrin formulation	2.4-fold improvement in bioavailability ⁹³
	Norfloxacin	Rabbits	Crystalline form of Norfloxacin	1.4-fold improvement in bioavailability ⁹⁴
			Cyclodextrin formulation	Almost similar bioavailability ⁹⁴
PEG-6000 (with/without polysorbate 80 and oleic acid)	Ketoconazole		Crystalline form of Ketoconazole	5.5-fold improvement in bioavailability ⁹⁵
			With vs. without polysorbate 80 and oleic acid	2.7-fold improvement in bioavailability ⁹⁵
PEG-6000 (with/without TGPS and Gelucire 44/14)	Halofantrine	Dogs	IV Halofantrine	5 to 7- fold improvement in bioavailability ⁹⁶
			With vs. without surfactants	Almost similar bioavailability ⁹⁶
PEG-8000	Ritonavir	Dogs	Crystalline form of ritonavir	10 to 22-fold improvement in AUC and bioavailability ⁹⁷
PVP	BMS-488043	Dogs	Crystalline form of BMS-488043	15 to 18-fold improvement in C _{max} and 7 to 9-fold improvement in AUC ⁹⁸
	Frusemide	Humans	Crystalline form of frusemide	Shorter Tmax and slight improvement in bioavailability ⁹⁹
	KRN633	Mice	Crystalline form of KRN633	7.5-fold improvement in bioavailability ¹⁰⁰
	Lonidamine	Rats	Crystalline form of lonidamine	1.9-fold increase in AUC ⁹¹
			Cyclodextrin formulation	Almost similar bioavailability ⁹¹
Tolbutamide	Dogs	Cyclodextrin formulation before storage	Almost similar bioavailability ¹⁰¹	

			Cyclodextrin formulation after storage (one week at 60C and 75%RH)	3-fold reduction in bioavailability ¹⁰¹
PVP (with/without sodium caprate (SC))	Oleanolic acid	Rats	Commercial Oleic acid	Improvement in bioavailability ¹⁰²
			With vs. without SC	Without SC was superior to with SC ¹⁰²
PVP/VA	Nimodipine	Dogs	Nimodipine powder	2.3-fold improvement in bioavailability ¹⁰³
			Nimotop®	1.2-fold reduction in bioavailability ¹⁰³
PVAP	Itraconazole (1:2)	Rats	Sporanox®	Reduction in bioavailability, AUC decreased by 6-fold ⁸⁸
HPMC	Itraconazole	Rats	Sporanox®	Almost similar C _{max} , AUC and bioavailability ¹⁰⁴
	Irbesartan	Rabbits	Irbesartan suspension	1.8-fold improvement in C _{max} and bioavailability ¹⁰⁵
	Nimodipine	Dogs	Nimodipine powder	2-fold improvement in bioavailability ¹⁰³
			Nimotop®	1.4-fold reduction in bioavailability ¹⁰³
Tacrolimus	Dogs	Crystalline form of tacrolimus	10 fold improvement in AUC and bioavailability ¹⁰⁶	
HPMC and HPMCP	Albendazole	Rabbits	Albendazole and lactose mixture	1.4 to 3-fold improvement in bioavailability ¹⁰⁷
HPMC and poloxamer 407	Ibuprofen	Rats	Ibuprofen powder	9-fold improvement in AUC and bioavailability ¹⁰⁸
HPMC and SLS	Valsartan	Rats	Valsartan powder	Higher C _{max} , shorter T _{max} and 2.2-fold improvement in bioavailability ¹⁰⁹
			Diovan®	Higher C _{max} , shorter T _{max} and 1.7-fold improvement in bioavailability ¹⁰⁹
HPMCAS	AMG517	Monkeys	OraPlus suspension (cocrystals suspension)	1.5-fold improvement in C _{max} and 1.6-fold improvement in bioavailability ¹¹⁰
	Vemurafenib	Humans	Crystalline form of vemurafenib	4.4 to 4.7 improvement in bioavailability ¹¹¹
Eudragit E100 (polymethacrylate-based)	Fenofibrate	Dogs	Lipanthyl®	1.2-fold improvement in AUC and bioavailability ¹¹²
Eudragit EPO (polymethacrylate-based)	Tranilast	Rats	Crystalline form of tranilast	19-fold improvement in bioavailability ¹¹³
Eudragit EPO (polymethacrylate-based)	Nimodipine	Dogs	Nimodipine powder	3-fold improvement in bioavailability ¹⁰³
			Nimotop®	Almost similar bioavailability ¹⁰³

Table (3) Summarized list of widely investigated polymers combined with various APIs in amorphous solid dispersions, and their brief concluded in vivo bioavailability outcome.

6. Influence of manufacturing methods on amorphous solid dispersions

The dissolution rate and the bioavailability of the amorphous solid dispersions are strongly influenced by the physicochemical properties of API and carrier, as well as the used production process.^{114,115} Therefore, to obtain a product with desirable attributes, both the formulation and production procedures should be carefully considered. Various methods of preparation of amorphous solid dispersions have been introduced and developed over the years, and many studies have investigated their impact on performance at both physical and clinical aspects. These techniques can be categorized according to their principle of action to thermal-based procedures and solvent evaporation based-procedures. The thermal-based methods are the simple fusion method and the hot melt extrusion. On the other hand, solvent evaporation-based methods include spray-drying, freeze-drying, and supercritical fluid precipitation/extraction. An overview of each procedure, its advantages and disadvantages are summarized in table (4).

Owing to their low melting point, PEGs were the most commonly used polymers of the simple fusion methods.^{89,116–119} The fusion method offers potential usefulness in screening various model APIs or polymers quickly and at low cost. Often when compared to the other advanced methods, this method demonstrated lower dissolution rates and bioavailability results.^{93,120} However 'KinetiSol® Dispersing', which is an upgraded non-solvent fusion-based process,¹²¹ showed superiority over hot melt extrusion in terms of reduced processing temperatures and shortened residence times, therefore more suitable for a heat-sensitive API such as hydrocortisone.¹²² Other examples of comparing the different methods were reported in the literature. Mahlin et al. tested the glass forming ability (amorphization) of sixteen poorly soluble APIs, using different production procedures.¹²³ Only half of them produced amorphous forms by spray-drying and melt-quenching (fusion). Additionally, sulfamerazine and tolazamide were glass-formers only by melt-quenching, and not by spray-drying. Solid dispersions different API-polymer ratios of miconazole using copolymer of PEG and polyvinyl alcohol (PEG-PVA) were prepared using hot melt extrusion and spray-drying methods.¹²⁴ Results showed that all solid dispersions prepared by spray-drying displayed two T_g s, indicating that miconazole was miscible with the PEG fraction of the copolymer and not miscible with the PVA fraction, leading to crystallization of miconazole. Alternatively, by hot melt extrusion process, only one T_g was detected and mixing capacity was much higher. Furthermore, spray-drying was compared to anti-solvent supercritical fluid in the preparation of amorphous atorvastatin hemi-calcium.¹²⁵ Owing to more particle size reduction and narrow particle size distribution, the anti-solvent critical fluid method had demonstrated better dissolution rates and bioavailability than the spray-drying-method. In overall, a better theoretical and practical understanding of the influence of each method conditions on the final product is required.

Methodology	Pros	Cons
<p style="text-align: center;">Fusion method¹¹⁴</p> <ul style="list-style-type: none"> • Simple classic process in which the API is physically mixed with the molten carrier. • Rapid cooling with stirring until solidification. • Dry powder is obtained from the solid mass by means of crushing, milling, and/or sieving. • Commonly used carriers are PEGs due to their low melting points. 	<ul style="list-style-type: none"> • Simplicity and relative quickness. • Useful for initial wide screening of formulations and carriers in the lab. 	<ul style="list-style-type: none"> • Only APIs and polymers with low T_m. • Hard texture of the solid dispersion after cooling, therefore particle size reduction is impractical. • Irreproducible on large scale. • When tested, usually provides the least physically stable results and lowest dissolution rates and bioavailability compared to other methods.
<p style="text-align: center;">Hot melt extrusion^{126,127}</p> <ul style="list-style-type: none"> • A combination of melting and mechanical sheering. • The feed is pumped through a hopper to a heating barrel where the thermal energy is generated by both the sheering forces of the rotating screws and electric heating bands. • The co-melt is then extruded through an end-plate die. • Finally downstream processing where rapid cooling, rolling, or molding takes place. • Commonly used carriers are HPMC, PVP and PVPAC. 	<ul style="list-style-type: none"> • Reproducible on large scale. • Improved dissolution rates were reported. • Better controlled temperature system than fusion method. 	<ul style="list-style-type: none"> • Only APIs and polymers with low T_m. • Often unstable under severe storage conditions.
<p style="text-align: center;">Spray drying¹¹⁵</p> <ul style="list-style-type: none"> • A solvent evaporation-based method to transform a solution or a suspension into a solid dry product by rapidly drying with a gas. • Initial atomization of the liquid into very fine droplets by applying pressure, thus increasing the overall surface area. • This pressure or energy applied ranges from centrifugal energy through rotary atomizers, or kinetic energy by applying pressurized air through pneumatic or bi-fluid nozzles, to vibrational energy by ejecting the liquid stream through ultrasonic nozzles utilizing a micron-sized spray mesh technique. • Afterwards, the droplets are mixed with the drying gas mostly in a co-current stream, usually air or sometimes nitrogen if the liquid is organic or oxygen sensitive. • Finally, the solute or the dispersed API is separated from the evaporated solvent and collected by a cyclone system as solid dry powder. 	<ul style="list-style-type: none"> • Reproducible on large scale and high production output can be achieved. • Does not comprise melting, therefore avoids any possible thermal degradation of the API or the carrier. • Suitable for a wide variety of polymers and with utilizing a multi-carrier/polymer system. • Particle size reduction is facilitated. 	<ul style="list-style-type: none"> • Certain amounts of residual solvent(s) is usually detected in the final product, therefore any use of toxic solvents must be precluded. • Sometimes, residual sticky products are formed at the outlet of the spray drier. This is usually encountered when T_g of the products is lower than the outlet temperature, meaning they will exist in the rubbery sticky state during exiting.
<p style="text-align: center;">Freeze drying^{114,128}</p> <ul style="list-style-type: none"> • Another solvent evaporation-based method. • Initially, the API together with the solvent, 	<ul style="list-style-type: none"> • Reproducible on large scale and high production 	<ul style="list-style-type: none"> • High cost and time consuming.

carrier and excipients are freeze dried by liquid nitrogen until solidification.

- By cooling rapidly enough, no crystallization takes place until T_g is reached and the mobility of the molecules is strongly reduced, eventually forming glass.
- Afterwards a process of primary drying is performed, where the pressure is reduced and solvent is removed by sublimation.
- Further secondary drying is then performed, where the temperature is gradually raised to ambient temperature, and pressure is further decreased to remove the unfrozen solvent by desorption and eliminate any traces of moisture.
- output can be achieved.
- Does not comprise melting, therefore avoids any possible thermal degradation of the API or the carrier.
- Suitable for a wide variety of polymers and with utilizing a multi-carrier/polymer system.

Supercritical fluid precipitation/extraction^{114,129}

- The process of extracting solvents from the system by supercritical fluids, which is a fluid that is pressurized above its critical pressure (P_c) and heated above its critical temperature (T_c). CO₂ is the most commonly used supercritical fluid. It can act as a solvent or anti-solvent.
- In the first case, the API is dissolved in the supercritical fluid itself, sprayed through a nozzle into a chamber of reduced pressure and temperature, leading to the precipitation out of the API, purely or dispersed in a carrier system.
- For the second case, the API and a carrier are dissolved in a co-solvent, and then the solution is saturated with the supercritical fluid, leading to decreased solubility of the API and the carrier in the solvent and therefore extraction/precipitation out of the solvent.
- Low cost, simplicity, and quickness.
- Improved dissolution rates were reported.
- CO₂ is cheap, non-toxic and recyclable after processing.
- CO₂, the commonly used supercritical fluid has a limited dissolving power, therefore usually cannot be used as a solvent in the extraction procedure.
- For CO₂ to act as anti-solvent, both the API and the carrier must be soluble only in the solvent, and not soluble in the supercritical CO₂-solvent miscible mixture, which again limits the available choices of the API and the carrier in application.
- Crystallization at higher drug loading ratios was often reported.
- Residual amounts of solvent were often detected.

Table (4) A summary of commonly-used manufacturing procedures for amorphous solid dispersions, demonstrating their corresponding advantages and disadvantages.

7. Summary and conclusion

Since the vast majority of emerging new molecular entities are poorly-water soluble drug substance, the pharmaceutical industry consensus has been dedicated over the years towards developing formulations resolving these solubility challenges. This unstoppable increase in the number of poorly water-soluble drug candidates could be attributed to the persistent trend towards higher molecular weight and more lipophilic predicted drug design, which is not disappearing in the foreseeable future. Options developed to address this issue have evolved from conventional reduction in the particle size, or chemical modifications as salt forms and prodrugs, to formulary solutions of lipid formulations and amorphous dispersions. For all these introduced formulations including amorphous solid dispersions, it has been shown that there are both potential benefits along with considerable technical challenges that need to be sorted out.

When preparing amorphous solid dispersions, there are two main significant issues to consider. First, how long the system can maintain physicochemical stability over the expected shelf life before it might eventually relax and convert back to the more stable and favorable crystalline state? The second uncertainty is whether the amorphous form will be dispersed as a supersaturated solution after being administered and consequently displaying appropriate therapeutic effectiveness as bioavailability and bioactivity.

To address these queries raised above, several facts should be taken in considerations when experimenting on solid amorphous solid dispersions. To begin with, many studies have shown that amorphous solid dispersions prepared by the described methods are stable in short-term stability studies (3-6 months), however long-term stability is still lacking in most cases due to logistical difficulties. Actually one of the fundamental problem facing physical stability experiments has been always time related, and therefore there is a need for a well-established model to predict the onset of crystallization on time-basis. Despite the enormous data reported on amorphous solid dispersion, there are still issues associated with establishment and characterization of acceptable amorphous stable systems. Better understanding of the crystallization process in organic molecules, both at the surface and in the bulk, is still needed as many factors seem to be involved. Therefore, establishing a coherent theoretical perspective on the supercooled liquids and glasses that clarifies their idiosyncratic complex behavior near the glass transition is essential. There are various debates in the literature of whether the crystal growth process would only be temperature dependant related to the T_g of the API, or related to other molecular structure, configuration and hydrogen bonding factors. Even far below T_g , studies have revealed that there is still a degree of molecular mobility that might be sufficient - in some cases - to jeopardize the stability of the system and promote nucleation and crystal growth. This suggests and approves the fact that the onset of crystallization is a complex thermodynamic process; therefore interpretation of the physical stability data of each API and its carrier system should be dealt with separately.

Formulation of amorphous APIs in polymer dispersions has been the most preferable method to improve their stability, and enhance their wettability and dissolution. Polymers have been shown to

inhibit crystallization in the bulk, but their impact on crystallization on the surface is much less. Since organic molecules have been shown to be more prone to surface crystal growth, more studies addressing polymers impact on the onset of surface crystallization needs to be performed. In general the choice of the most suitable polymer for a certain API requires a coordinated methodical process of screening. The analysis of the data collected and represented in table (3) reveals the wide extent of investigation directed towards an API-polymer combined system to produce stable and effective amorphous solid dispersions. Moreover, the data supports the practical advantages postulated when a polymer is co-formulated with a poorly water-soluble API, and the impact on its pharmaceutical performance in terms of dissolution and bioavailability improvement. Almost all of API-polymer amorphous dispersions have demonstrated superior bioavailability when compared to their crystalline counterparts. Others compared to solid dosage formulations as cyclodextrin complexes and co-crystals, or already marketed amorphous products; the results differed according to the polymer used and the ratio to the API. In addition, several studies have compared the addition of different polymers to a certain API, along with other factors being unified such as the methodology for preparation, and results usually were variable between the different polymer dispersions. Characteristics such as the T_g of the polymer, stereo-chemistry, molecular weight, and miscibility with the API can all affect the pharmaceutical outcome of the dispersion. Therefore, the API to polymer ratio should be optimized to provide the desired physical stability and attain favorable dissolution and bioavailability rates. Furthermore, the presence of surfactants acting as solubilizers and promoting dissolution at faster rates was apparent in most of the studies. Mesoporous systems were proven to stabilize amorphous dispersions against crystal growth, by reducing the free energy and limiting the molecular mobility in the system, as the API is dispersed on a relatively large surface area. Nanocoating was shown to limit surface crystallization along with maintaining favorable dissolution properties; however more data is required to comprehensively assess their performance on various API molecules. Perhaps a new strategy of combining both an API-polymer system with nanocoating might prove as a successful blockade for both modes of crystal growth.

Finally, the fate of any formulated product can be predicted using several *in vitro* and *in vivo* tests to investigate the effects of dispersion. Unfortunately there was a lack of systematic approach in some studies, where *in vivo* testing were directly conducted without establishing preliminary observations from *in vitro* or *in silico* experiments. In general, physiologically relevant factors, as dissolution media volume, simulated pH variations, simulated mixing and agitation and dissolution exposure times should all be optimized and tailored to mimic real GIT conditions. The selection of the species used in the *in vivo* experiments requires careful understanding of their differences such as GIT physiology, gastric and intestinal absorption, dietary effects and body index, and hence these related factors must be taken in consideration.

In conclusion, amorphous solid dispersions are well established delivery formulations addressing poor water solubility in pharmaceutical compounds, with a continuously growing number of products on the market. Their enhanced dissolution and bioavailability however, comes at a cost of having high metastable behavior and a tendency to recrystallize again. Much effort has been already done in stabilization strategies of amorphous dispersions and more interest is expected to be gained in the near

future. It is up to formulation and pharmaceutical industry experts to come up with more successful solutions addressing these problematic challenges associated with their stability and drug release characteristics.

8. References

1. Yu LX, Amidon GL, Polli JE, et al. Biopharmaceutics classification system: the scientific basis for biowaiver extensions. *Pharmaceutical research*. 2002;19(7):921–5. Available at: <http://www.ncbi.nlm.nih.gov/pubmed/12180542>.
2. Food and Drug Administration. Guidance for Industry: Waiver of In Vivo Bioavailability and Bioequivalence Studies for Immediate Release Solid Oral Dosage Forms Based on a Biopharmaceutics Classification System. 2000. Available at: <http://www.fda.gov/OHRMS/DOCKETS/98fr/3657gd3.pdf>.
3. Pouton CW. Formulation of poorly water-soluble drugs for oral administration: physicochemical and physiological issues and the lipid formulation classification system. *European journal of pharmaceutical sciences : official journal of the European Federation for Pharmaceutical Sciences*. 2006;29(3-4):278–87. Available at: <http://www.ncbi.nlm.nih.gov/pubmed/16815001>. Accessed July 11, 2014.
4. Amidon GL, Lennernäs H, Shah VP, Crison JR. A Theoretical Basis for a Biopharmaceutic Drug Classification: The Correlation of in Vitro Drug Product Dissolution and in Vivo Bioavailability. *Pharmaceutical Research*. 1995;12(3):413–420. Available at: <http://www.ncbi.nlm.nih.gov/pubmed/7617530>.
5. Serajuddin ATM. Salt formation to improve drug solubility. *Advanced drug delivery reviews*. 2007;59(7):603–16. Available at: <http://www.ncbi.nlm.nih.gov/pubmed/17619064>. Accessed May 23, 2014.
6. Rasenack N, Müller BW. Micron-size drug particles: common and novel micronization techniques. *Pharmaceutical development and technology*. 2004;9(1):1–13. Available at: <http://www.ncbi.nlm.nih.gov/pubmed/15000462>. Accessed June 1, 2014.
7. Serajuddin AT. Solid dispersion of poorly water-soluble drugs: early promises, subsequent problems, and recent breakthroughs. *Journal of pharmaceutical sciences*. 1999;88(10):1058–66. Available at: <http://www.ncbi.nlm.nih.gov/pubmed/10514356>.
8. Merisko-Liversidge E, Liversidge GG, Cooper ER. Nanosizing: a formulation approach for poorly-water-soluble compounds. *European journal of pharmaceutical sciences : official journal of the European Federation for Pharmaceutical Sciences*. 2003;18(2):113–20. Available at: <http://www.ncbi.nlm.nih.gov/pubmed/12594003>.
9. Kesisoglou F, Panmai S, Wu Y. Nanosizing--oral formulation development and biopharmaceutical evaluation. *Advanced drug delivery reviews*. 2007;59(7):631–44. Available at: <http://www.ncbi.nlm.nih.gov/pubmed/17601629>. Accessed June 6, 2014.
10. Cassidy a MC, Gardner CE, Jones W. Following the surface response of caffeine cocrystals to controlled humidity storage by atomic force microscopy. *International journal of pharmaceutics*. 2009;379(1):59–66. Available at: <http://www.ncbi.nlm.nih.gov/pubmed/19539735>. Accessed July 18, 2014.

11. Pouton CW. Formulation of self-emulsifying drug delivery systems. *Advanced Drug Delivery Reviews*. 1997;25(1):47–58. Available at: <http://www.sciencedirect.com/science/article/pii/S0169409X96004905>.
12. Pouton CW. Lipid formulations for oral administration of drugs: non-emulsifying, self-emulsifying and “self-microemulsifying” drug delivery systems. *European journal of pharmaceutical sciences : official journal of the European Federation for Pharmaceutical Sciences*. 2000;11 Suppl 2:S93–8. Available at: <http://www.ncbi.nlm.nih.gov/pubmed/11033431>.
13. Gursoy RN, Benita S. Self-emulsifying drug delivery systems (SEDDS) for improved oral delivery of lipophilic drugs. *Biomedicine & pharmacotherapy = Biomédecine & pharmacothérapie*. 2004;58(3):173–82. Available at: <http://www.ncbi.nlm.nih.gov/pubmed/15082340>. Accessed May 30, 2014.
14. Pouton CW, Porter CJH. Formulation of lipid-based delivery systems for oral administration: materials, methods and strategies. *Advanced drug delivery reviews*. 2008;60(6):625–37. Available at: <http://www.ncbi.nlm.nih.gov/pubmed/18068260>. Accessed June 15, 2014.
15. Brouwers J, Brewster ME, Augustijns P. Supersaturating Drug Delivery Systems : The Answer to Solubility-Limited Oral Bioavailability ? *Journal of Pharmaceutical Sciences*. 2009;98(8):2549–2572. Available at: <http://www.ncbi.nlm.nih.gov/pubmed/19373886>.
16. Hancock BC, Zografi G. Characteristics and significance of the amorphous state in pharmaceutical systems. *Journal of pharmaceutical sciences*. 1997;86(1):1–12. Available at: <http://www.ncbi.nlm.nih.gov/pubmed/9002452>.
17. Zarzycki J. Glasses and the Vitreous State. *Cambridge University Press*. 1991. Available at: <http://www.cambridge.org/us/academic/subjects/engineering/materials-science/glasses-and-vitreous-state?format=HB>.
18. Angell CA. Structural instability and relaxation in liquid and glassy phases near the fragile liquid limit. *Journal of Non-Crystalline Solids*. 1988;102(1-3):205–221. Available at: <http://www.sciencedirect.com/science/article/pii/0022309388901330>.
19. Ediger MD, Angell CA, Nagel SR. Supercooled Liquids and Glasses. *Journal of physical chemistry*. 1996;100(31):13200–13212. Available at: <http://pubs.acs.org/doi/abs/10.1021/jp953538d>.
20. Debenedetti PG, Stillinger FH. Supercooled liquids and the glass transition. *Nature*. 2001;410(6825):259–67. Available at: <http://www.ncbi.nlm.nih.gov/pubmed/11258381>.
21. Angell C a. Formation of glasses from liquids and biopolymers. *Science (New York, N.Y.)*. 1995;267(5206):1924–35. Available at: <http://www.ncbi.nlm.nih.gov/pubmed/17770101>.
22. Mansfield ML. Model of the glass transition. *The Journal of Chemical Physics*. 1995;103(18):8124–8129. Available at: <http://scitation.aip.org/content/aip/journal/jcp/103/18/10.1063/1.470176>. Accessed July 8, 2014.
23. Brüning R, Samwer K. Glass transition on long time scales. *The American physical society*. 1992;46(18):318–322. Available at: <http://journals.aps.org/prb/abstract/10.1103/PhysRevB.46.11318>.

24. Bosma M, Brinke G, Ellist TS. Polymer-Polymer Miscibility and Enthalpy Relaxations. *Macromolecules*. 1988;21(5):1465–1470. Available at: <http://pubs.acs.org/doi/abs/10.1021/ma00183a041>.
25. Kauzmann W. The Nature of the Glassy State and the Behavior of Liquids at Low Temperatures. *Chemical Reviews*. 1948;43(2):219–256. Available at: <http://pubs.acs.org/doi/abs/10.1021/cr60135a002>.
26. Speedy RJ. Kauzmann 's paradox and the glass transition. *Biophysical Chemistry*. 2003;105(September 2002):411–420. Available at: <http://www.sciencedirect.com/science/article/pii/S0301462203001054#BIB13>.
27. Yoshioka M, Hancock BC, Zografi G. Crystallization of indomethacin from the amorphous state below and above its glass transition temperature. *Journal of pharmaceutical sciences*. 1994;83(12):1700–5. Available at: <http://www.ncbi.nlm.nih.gov/pubmed/7891297>.
28. Slade L, Levine H. Glass Transitions and Water-Food Structure Interactions. *Advances in Food and Nutrition Research*. 1995;38:103–269. Available at: <http://www.sciencedirect.com/science/article/pii/S1043452608600844#>.
29. Van Santen RA. The Ostwald step rule. *The Journal of Physical Chemistry*. 1984;88(24):5768–5769. Available at: <http://pubs.acs.org/doi/abs/10.1021/j150668a002>.
30. Pikal MJ, Lukes AL, Lang JE, Gaines K. Quantitative crystallinity determinations for β -lactam antibiotics by solution calorimetry: Correlations with stability. *Journal of pharmaceutical sciences*. 1978;67(6):767–773. Available at: <http://onlinelibrary.wiley.com/doi/10.1002/jps.2600670609/abstract>.
31. Ahlneck C, Zografi G. The molecular basis of moisture effects on the physical and chemical stability of drugs in the solid state. *International journal of pharmaceutics*. 1990;62:87–95. Available at: <http://www.sciencedirect.com/science/article/pii/0378517390902210>.
32. Slade L, Levine H. Non-equilibrium behavior of small carbohydrate-water systems. *Pure and Applied Chemistry*. 1988;60(12):1841–1864. Available at: <http://pac.iupac.org/publications/pac/60/12/1841/>.
33. Makower B, Dye WB. Equilibrium Moisture Content and Crystallization of Amorphous Sucrose and Glucose. *Journal of agricultural and food chemistry*. 1956;4(1):72–77. Available at: <http://pubs.acs.org/doi/abs/10.1021/jf60059a010>.
34. IMAIZUMI H, NAMBU N, NAGAI T. Stability and Several Physical Properties of Amorphous and Crystalline Forms of Indomethacin. *Pharmaceutical Society of Japan*. 1980;28:2565–2569. Available at: https://www.jstage.jst.go.jp/article/cpb1958/28/9/28_9_2565/_article.
35. Andronis V, Yoshioka M, Zografi G. Effects of sorbed water on the crystallization of indomethacin from the amorphous state. *Journal of pharmaceutical sciences*. 1997;86(3):346–51. Available at: <http://www.ncbi.nlm.nih.gov/pubmed/9050804>.

36. Gordon M, Taylor JS. Ideal copolymers and the second-order transitions of synthetic rubbers. i. non-crystalline copolymers. *Journal of Applied Chemistry*. 1952;2(9):439–500. Available at: <http://onlinelibrary.wiley.com/doi/10.1002/jctb.5010020901/abstract>.
37. Mullin JW. Crystallization: 4th edition. *Elsevier Butterworth-Heinemann*. 2001. Available at: <http://www.sciencedirect.com/science/book/9780750648332>.
38. Zanutto ED, James PF. Experimental tests of the classical nucleation theory for glasses. *Journal of Non-Crystalline Solids*. 1985;74(2-3):373–394. Available at: <http://linkinghub.elsevier.com/retrieve/pii/0022309385900808>.
39. Laidler KJ. The Development of the Arrhenius Equation. *Journal of chemical education*. 1984;61(6):494–498. Available at: <http://pubs.acs.org/doi/abs/10.1021/ed061p494>.
40. Bhugra C, Pikal MJ. Role of Thermodynamic , Molecular , and Kinetic Factors in Crystallization From the Amorphous State. *Journal of pharmaceutical sciences*. 2008;97(4):1329–1349. Available at: <http://onlinelibrary.wiley.com.proxy.library.uu.nl/doi/10.1002/jps.21138/full>.
41. Cheng SZD, Lotz B. Enthalpic and entropic origins of nucleation barriers during polymer crystallization: the Hoffman–Lauritzen theory and beyond. *Polymer*. 2005;46(20):8662–8681. Available at: <http://linkinghub.elsevier.com/retrieve/pii/S0032386105007159>. Accessed July 11, 2014.
42. Avrami M. Kinetics of Phase Change. II Transformation-Time Relations for Random Distribution of Nuclei. *The Journal of Chemical Physics*. 1940;8(2):212. Available at: <http://scitation.aip.org/content/aip/journal/jcp/8/2/10.1063/1.1750631>. Accessed July 11, 2014.
43. Williams G, Watts DC. Non-Symmetrical Dielectric Relaxation Behaviour Arising from a Simple Empirical Decay Function. *Transactions of the Faraday Society*. 1970;66:80–85. Available at: <http://pubs.rsc.org/en/Content/ArticleLanding/1970/TF/TF9706600080#!divAbstract>.
44. Marsac PJ, Konno H, Taylor LS. A Comparison of the Physical Stability of Amorphous Felodipine and Nifedipine Systems. *Pharmaceutical research*. 2006;23(10):2306–2316.
45. Cowie JMG, Ferguson R. Physical aging studies in polymer blends. 2. Enthalpy relaxation as a function of aging temperature in a poly(vinyl methyl ether)/polystyrene blend. *Macromolecules*. 1989;22(5):2312–2317. Available at: <http://pubs.acs.org/doi/abs/10.1021/ma00195a054>.
46. Shamblin SL, Zografi G. Enthalpy relaxation in binary amorphous mixtures containing sucrose. *Pharmaceutical research*. 1998;15(12):1828–1834. Available at: <http://www.ncbi.nlm.nih.gov/pubmed/9892465>.
47. Koster UWE. Surface Crystallization of Metallic Glasses. *Materials Science and Engineering*. 1988;97:233–239. Available at: <http://www.sciencedirect.com/science/article/pii/0025541688900493#>.
48. Wu T, Yu L. Surface crystallization of indomethacin below T_g. *Pharmaceutical research*. 2006;23(10):2350–5. Available at: <http://www.ncbi.nlm.nih.gov/pubmed/16927184>. Accessed July 1, 2014.

49. Eihei F, Midori M, Shigeo Y. Glassy state of pharmaceuticals. III. Thermal properties and stability of glassy pharmaceuticals and their binary glass systems. *Chemical & pharmaceutical bulletin*. 1989;37(4):1047–1050. Available at: <http://ci.nii.ac.jp/naid/110003627672>.
50. Sun Y, Zhu L, Kearns KL, Ediger MD, Yu L. Glasses crystallize rapidly at free surfaces by growing crystals upward. *Proceedings of the National Academy of Sciences of the United States of America*. 2011;108(15):5990–5. Available at: <http://www.pubmedcentral.nih.gov/articlerender.fcgi?artid=3076810&tool=pmcentrez&rendertype=abstract>. Accessed July 11, 2014.
51. Zhu L, Wong L, Yu L. Surface-enhanced crystallization of amorphous nifedipine. *Molecular pharmaceutics*. 2008;5(6):921–6. Available at: <http://www.ncbi.nlm.nih.gov/pubmed/19434917>.
52. Miyazaki T, Yoshioka S, Aso Y, Kawanishi T. Crystallization rate of amorphous nifedipine analogues unrelated to the glass transition temperature. *International journal of pharmaceutics*. 2007;336(1):191–5. Available at: <http://www.ncbi.nlm.nih.gov/pubmed/17184940>. Accessed July 10, 2014.
53. Brian CW, Yu L. Surface self-diffusion of organic glasses. *The journal of physical chemistry. A*. 2013;117(50):13303–9. Available at: <http://www.ncbi.nlm.nih.gov/pubmed/23829661>.
54. Diaz-Mora N, Zanotto ED, Hergt R, Müller R. Surface crystallization and texture in cordierite glasses. *Journal of Non-Crystalline Solids*. 2000;273(1-3):81–93. Available at: <http://linkinghub.elsevier.com/retrieve/pii/S0022309300001472>.
55. Wittman E, Zanotto ED. Surface nucleation and growth in Anorthite glass. *Journal of Non-Crystalline Solids*. 2000;271(1-2):94–99. Available at: <http://linkinghub.elsevier.com/retrieve/pii/S0022309300000855>.
56. Bell RC, Wang H, Iedema MJ, Cowin JP. Nanometer-resolved interfacial fluidity. *Journal of the American Chemical Society*. 2003;125(17):5176–85. Available at: <http://www.ncbi.nlm.nih.gov/pubmed/12708869>.
57. Wu T, Sun Y, Li N, de Villiers MM, Yu L. Inhibiting surface crystallization of amorphous indomethacin by nanocoating. *Langmuir : the ACS journal of surfaces and colloids*. 2007;23(9):5148–53. Available at: <http://www.ncbi.nlm.nih.gov/pubmed/17397203>.
58. Vallet-Regí M. Ordered mesoporous materials in the context of drug delivery systems and bone tissue engineering. *Chemistry (Weinheim an der Bergstrasse, Germany)*. 2006;12(23):5934–43. Available at: <http://www.ncbi.nlm.nih.gov/pubmed/16832799>. Accessed July 14, 2014.
59. Yiu HHP, Wright P a. Enzymes supported on ordered mesoporous solids: a special case of an inorganic–organic hybrid. *Journal of Materials Chemistry*. 2005;15(35-36):3690. Available at: <http://xlink.rsc.org/?DOI=b506090g>. Accessed July 14, 2014.
60. Qian KK, Bogner RH. Application of Mesoporous Silicon Dioxide and Silicate in Oral Amorphous Drug Delivery Systems. *Journal of pharmaceutical sciences*. 2012;101(2):444–463. Available at: <http://www.ncbi.nlm.nih.gov/pubmed/21976048>.

61. Sing KSW. Reporting physisorption data for gas/solid systems with special reference to the determination of surface area and porosity. *Pure and Applied Chemistry*. 1982;54(11):2201–2218. Available at: <http://pac.iupac.org/publications/pac/pdf/1982/pdf/5411x2201.pdf>.
62. Jackson CL, Mckenna GB. Vitrification and Crystallization of Organic Liquids Confined to Nanoscale Pores. *Chemistry of Materials*. 1996;8(8):2128–2137. Available at: <http://pubs.acs.org/doi/abs/10.1021/cm9601188>.
63. Speybroeck M Van, Barillaro RY, Thi TDO, et al. Ordered Mesoporous Silica Material SBA-15 : A Broad-Spectrum Formulation Platform for Poorly Soluble Drugs. *Journal of Pharmaceutical Sciences*. 2009;98(8):2648–2658. Available at: <http://www.ncbi.nlm.nih.gov/pubmed/19072861>.
64. Limnell T, Heikkilä T, Santos H a, et al. Physicochemical stability of high indomethacin payload ordered mesoporous silica MCM-41 and SBA-15 microparticles. *International journal of pharmaceutics*. 2011;416(1):242–51. Available at: <http://www.ncbi.nlm.nih.gov/pubmed/21763766>. Accessed July 14, 2014.
65. Shen S, Ng WAIK, Chia L, Dong Y, Tan RBH. Stabilized Amorphous State of Ibuprofen by Co-Spray Drying With Mesoporous SBA-15 to Enhance Dissolution Properties. *Journal of Pharmaceutical Sciences*. 2010;99(4):1997–2007. Available at: <http://onlinelibrary.wiley.com/doi/10.1002/jps.21967/full>.
66. Mellaerts R, Aerts C a, Van Humbeeck J, Augustijns P, Van den Mooter G, Martens J a. Enhanced release of itraconazole from ordered mesoporous SBA-15 silica materials. *Chemical communications (Cambridge, England)*. 2007;7(13):1375–1377. Available at: <http://www.ncbi.nlm.nih.gov/pubmed/17377687>. Accessed July 14, 2014.
67. Sauvageot CM-E, Weatherbee JL, Kesari S, et al. Efficacy of the HSP90 inhibitor 17-AAG in human glioma cell lines and tumorigenic glioma stem cells. *Neuro-oncology*. 2009;11(2):109–21. Available at: <http://www.pubmedcentral.nih.gov/articlerender.fcgi?artid=2718982&tool=pmcentrez&rendertype=abstract>. Accessed July 10, 2014.
68. Zhang Y, Jiang T, Zhang Q, Wang S. Inclusion of telmisartan in mesocellular foam nanoparticles: drug loading and release property. *European journal of pharmaceutics and biopharmaceutics : official journal of Arbeitsgemeinschaft für Pharmazeutische Verfahrenstechnik e.V.* 2010;76(1):17–23. Available at: <http://www.ncbi.nlm.nih.gov/pubmed/20685333>. Accessed July 14, 2014.
69. Mellaerts R, Mols R, Jammaer J a G, et al. Increasing the oral bioavailability of the poorly water soluble drug itraconazole with ordered mesoporous silica. *European journal of pharmaceutics and biopharmaceutics : official journal of Arbeitsgemeinschaft für Pharmazeutische Verfahrenstechnik e.V.* 2008;69(1):223–30. Available at: <http://www.ncbi.nlm.nih.gov/pubmed/18164930>. Accessed July 14, 2014.
70. Van Speybroeck M, Mols R, Mellaerts R, et al. Combined use of ordered mesoporous silica and precipitation inhibitors for improved oral absorption of the poorly soluble weak base itraconazole. *European journal of pharmaceutics and biopharmaceutics : official journal of Arbeitsgemeinschaft für Pharmazeutische Verfahrenstechnik e.V.* 2010;75(3):354–65. Available at: <http://www.ncbi.nlm.nih.gov/pubmed/20420905>. Accessed July 14, 2014.

71. Newman A, Knipp G, Zografi G. Assessing the Performance of Amorphous Solid Dispersions. *Journal of Pharmaceutical Sciences*. 2012;101(4):1355–1377. Available at: <http://onlinelibrary.wiley.com/doi/10.1002/jps.23031/full>.
72. Newman A, Engers D, Bates S, Ivanisevic I, Kelly RC, Zografi G. Characterization of Amorphous API : Polymer Mixtures Using X-Ray Powder Diffraction. *Journal of pharmaceutical sciences*. 2008;97(11):4840–4856. Available at: <http://www.ncbi.nlm.nih.gov/pubmed/18351626>.
73. Shamblin SL, Taylor LS, Zografi G. Mixing behavior of colyophilized binary systems. *Journal of pharmaceutical sciences*. 1998;87(6):694–701. Available at: <http://www.ncbi.nlm.nih.gov/pubmed/9607945>.
74. Tao J, Sun Y, Zhang GGZ, Yu L. Solubility of small-molecule crystals in polymers: D-mannitol in PVP, indomethacin in PVP/VA, and nifedipine in PVP/VA. *Pharmaceutical research*. 2009;26(4):855–64. Available at: <http://www.ncbi.nlm.nih.gov/pubmed/19052850>. Accessed July 9, 2014.
75. Sun YE, Tao J, Zhang GGZ, Yu L. Solubilities of Crystalline Drugs in Polymers : An Improved Analytical Method and Comparison of Solubilities of Indomethacin and Nifedipine in PVP , PVP / VA , and PVAc. *Journal of pharmaceutical sciences*. 2010;99(9):4023–4031. Available at: <http://www.ncbi.nlm.nih.gov/pubmed/20607809>.
76. Flory PJ. Principles of polymer chemistry. *Cornell University Press*. 1953. Available at: <http://www.cornellpress.cornell.edu/book/?GCOI=80140100145700>.
77. Taylor LS, Zografi G. Spectroscopic Characterization of Interactions Between PVP and Indomethacin in Amorphous Molecular Dispersions. *Pharmaceutical Research*. 1997;14(12):1691–1698. Available at: <http://www.ncbi.nlm.nih.gov/pubmed/9453055>.
78. Antonucci JM, Liu DW, Skrtic D. Amorphous Calcium Phosphate Based Composites: Effect of Surfactants and Poly(ethylene oxide) on Filler and Composite Properties. *Journal of dispersion science and technology*. 2005;28(5):819–824. Available at: <http://www.ncbi.nlm.nih.gov/pubmed/18714365>.
79. Mosquera-Giraldo LI, Trasi NS, Taylor LS. Impact of surfactants on the crystal growth of amorphous celecoxib. *International journal of pharmaceutics*. 2014;461(1-2):251–7. Available at: <http://www.ncbi.nlm.nih.gov/pubmed/24333451>. Accessed July 16, 2014.
80. Ghebremeskel AN, Vemavarapu C, Lodaya M. Use of surfactants as plasticizers in preparing solid dispersions of poorly soluble API: stability testing of selected solid dispersions. *Pharmaceutical research*. 2006;23(8):1928–36. Available at: <http://www.ncbi.nlm.nih.gov/pubmed/16871443>. Accessed July 16, 2014.
81. Honary S, Majidian A, Naghibi F. The Effect of Different Surfactants on Dissolution Rate of Recrystallized Indomethacin. *Iranian journal of pharmaceutical research*. 2007;6(1):25–33. Available at: http://ijpr.sbmu.ac.ir/article_695_6.html.
82. Curatolo W, Nightingale J a, Herbig SM. Utility of hydroxypropylmethylcellulose acetate succinate (HPMCAS) for initiation and maintenance of drug supersaturation in the GI milieu. *Pharmaceutical*

research. 2009;26(6):1419–31. Available at: <http://www.ncbi.nlm.nih.gov/pubmed/19277850>. Accessed July 15, 2014.

83. Bruno C, Hancock, Shamblin SL, Zografi G. Molecular Mobility of Amorphous Pharmaceutical Solids Below Their Glass Transition Temperatures. *Pharmaceutical Research*. 1995;12(6):799–806. Available at: <http://www.ncbi.nlm.nih.gov/pubmed/7667182>.

84. Matsumoto T, Zografi G. Physical Properties of Solid Molecular Dispersions of Indomethacin with Poly(vinylpyrrolidone) and Poly(vinylpyrrolidone-co-vinyl-acetate) in Relation to Indomethacin Crystallization. *Pharmaceutical Research*. 1999;16(11):1722–1728. Available at: <http://www.ncbi.nlm.nih.gov/pubmed/10571278>.

85. Powell CT, Cai T, Hasebe M, et al. Low-concentration polymers inhibit and accelerate crystal growth in organic glasses in correlation with segmental mobility. *The journal of physical chemistry. B*. 2013;117(35):10334–41. Available at: <http://www.ncbi.nlm.nih.gov/pubmed/23909486>.

86. Miyazaki T, Aso Y, Yoshioka S, Kawanishi T. Differences in crystallization rate of nitrendipine enantiomers in amorphous solid dispersions with HPMC and HPMCP. *International journal of pharmaceutics*. 2011;407(1-2):111–8. Available at: <http://www.ncbi.nlm.nih.gov/pubmed/21277962>. Accessed July 17, 2014.

87. Cai T, Zhu L, Yu L. Crystallization of organic glasses: effects of polymer additives on bulk and surface crystal growth in amorphous nifedipine. *Pharmaceutical research*. 2011;28(10):2458–66. Available at: <http://www.ncbi.nlm.nih.gov/pubmed/21638137>. Accessed July 18, 2014.

88. Dinunzio JC, Miller DA, Yang W, et al. Amorphous Compositions Using Concentration Enhancing Polymers for Improved Bioavailability of Itraconazole. *Molecular pharmaceutics*. 2008;5(6):968–980. Available at: <http://pubs.acs.org/doi/abs/10.1021/mp800042d>.

89. Joshi HN, Tejwani RW, Davidovich M, et al. Bioavailability enhancement of a poorly water-soluble drug by solid dispersion in polyethylene glycol–polysorbate 80 mixture. *International Journal of Pharmaceutics*. 2004;269(1):251–258. Available at: <http://linkinghub.elsevier.com/retrieve/pii/S0378517303004770>. Accessed July 12, 2014.

90. Xie Y, Xie P, Song X, Tang X, Song H. Preparation of esomeprazole zinc solid dispersion and study on its pharmacokinetics. *International journal of pharmaceutics*. 2008;360(1-2):53–7. Available at: <http://www.ncbi.nlm.nih.gov/pubmed/18495389>. Accessed July 17, 2014.

91. Palmieri GF, Cantalamessa F, Di Martino P, Nasuti C, Martelli S. Lonidamine solid dispersions: in vitro and in vivo evaluation. *Drug development and industrial pharmacy*. 2002;28(10):1241–50. Available at: <http://www.ncbi.nlm.nih.gov/pubmed/12476870>. Accessed July 17, 2014.

92. Law SL, Lo WY, Lin FM, Chaing CH. Dissolution and absorption of nifedipine in polyethylene glycol solid dispersion containing phosphatidylcholine. *International Journal of Pharmaceutics*. 1992;84(2):161–166. Available at: <http://linkinghub.elsevier.com/retrieve/pii/0378517392900568>.

93. Emara LH, Badr RM, Elbary a A. Improving the dissolution and bioavailability of nifedipine using solid dispersions and solubilizers. *Drug development and industrial pharmacy*. 2002;28(7):795–807. Available at: <http://www.ncbi.nlm.nih.gov/pubmed/12236065>. Accessed July 17, 2014.
94. F. Fawaz A, Boninia F, Guyota M, Bildeta J, Mauryb M, Laguenya AM. Bioavailability of norfloxacin from PEG 6000 solid dispersion and cyclodextrin inclusion complexes in rabbits. *International journal of pharmaceutics*. 1996;132(1-2):271–275. Available at: <http://www.sciencedirect.com/science/article/pii/037851739504387X>.
95. Heo M-Y, Piao Z-Z, Kim T-W, Cao Q-R, Kim A, Lee B-J. Effect of solubilizing and microemulsifying excipients in polyethylene glycol 6000 solid dispersion on enhanced dissolution and bioavailability of ketoconazole. *Archives of pharmacol research*. 2005;28(5):604–11. Available at: <http://www.ncbi.nlm.nih.gov/pubmed/15974450>.
96. Khoo SM, Porter CJ, Charman WN. The formulation of Halofantrine as either non-solubilizing PEG 6000 or solubilizing lipid based solid dispersions: physical stability and absolute bioavailability assessment. *International journal of pharmaceutics*. 2000;205(1-2):65–78. Available at: <http://www.ncbi.nlm.nih.gov/pubmed/11000543>.
97. Law D, Schmitt E a, Marsh KC, et al. Ritonavir-PEG 8000 amorphous solid dispersions: in vitro and in vivo evaluations. *Journal of pharmaceutical sciences*. 2004;93(3):563–70. Available at: <http://www.ncbi.nlm.nih.gov/pubmed/14762895>.
98. Fakes MG, Vakkalagadda BJ, Qian F, et al. Enhancement of oral bioavailability of an HIV-attachment inhibitor by nanosizing and amorphous formulation approaches. *International journal of pharmaceutics*. 2009;370(1-2):167–74. Available at: <http://www.ncbi.nlm.nih.gov/pubmed/19100319>. Accessed July 17, 2014.
99. Doherty C, York P. The in-vitro pH-dissolution dependence and in-vivo bioavailability of frusemide-PVP solid dispersions. *The Journal of pharmacy and pharmacology*. 1989;41(2):73–8. Available at: <http://www.ncbi.nlm.nih.gov/pubmed/2568431>.
100. Matsunaga N, Nakamura K, Yamamoto A, Taguchi E, Tsunoda H, Takahashi K. Improvement by solid dispersion of the bioavailability of KRN633, a selective inhibitor of VEGF receptor-2 tyrosine kinase, and identification of its potential therapeutic window. *Molecular cancer therapeutics*. 2006;5(1):80–8. Available at: <http://www.ncbi.nlm.nih.gov/pubmed/16432165>. Accessed July 17, 2014.
101. Kimura K, Hirayama F, Arima H, Uekama K. Effects of aging on crystallization, dissolution and absorption characteristics of amorphous tolbutamide-2-hydroxypropyl-beta-cyclodextrin complex. *Chemical & pharmaceutical bulletin*. 2000;48(5):646–50. Available at: <http://www.ncbi.nlm.nih.gov/pubmed/10823700>.
102. Tong HHY, Du Z, Wang GN, et al. Spray freeze drying with polyvinylpyrrolidone and sodium caprate for improved dissolution and oral bioavailability of oleanolic acid, a BCS Class IV compound. *International journal of pharmaceutics*. 2011;404(1-2):148–58. Available at: <http://www.ncbi.nlm.nih.gov/pubmed/21094233>. Accessed July 17, 2014.

103. Zheng X, Yang R, Zhang Y, Wang Z, Tang X, Zheng L. Part II: bioavailability in beagle dogs of nimodipine solid dispersions prepared by hot-melt extrusion. *Drug development and industrial pharmacy*. 2007;33(7):783–9. Available at: <http://www.ncbi.nlm.nih.gov/pubmed/17654027>. Accessed July 17, 2014.
104. Lee S, Nam K, Kim MS, et al. Preparation and characterization of solid dispersions of itraconazole by using aerosol solvent extraction system for improvement in drug solubility and bioavailability. *Archives of pharmacal research*. 2005;28(7):866–74. Available at: <http://www.ncbi.nlm.nih.gov/pubmed/16114503>.
105. Boghra RJ, Kothawade PC, Belgamwar VS, Nerkar PP, Tekade AR, Surana SJ. Solubility, dissolution rate and bioavailability enhancement of irbesartan by solid dispersion technique. *Chemical & pharmaceutical bulletin*. 2011;59(4):438–41. Available at: <http://www.ncbi.nlm.nih.gov/pubmed/21467670>.
106. Yamashita K, Nakate T, Okimoto K, et al. Establishment of new preparation method for solid dispersion formulation of tacrolimus. *International Journal of Pharmaceutics*. 2003;267(1-2):79–91. Available at: <http://linkinghub.elsevier.com/retrieve/pii/S0378517303004320>. Accessed July 17, 2014.
107. Kohri N, Yamayoshi Y, Xin H, et al. Improving the oral bioavailability of albendazole in rabbits by the solid dispersion technique. *The Journal of pharmacy and pharmacology*. 1999;51(2):159–64. Available at: <http://www.ncbi.nlm.nih.gov/pubmed/10217314>.
108. Park Y-J, Kwon R, Quan QZ, et al. Development of novel ibuprofen-loaded solid dispersion with improved bioavailability using aqueous solution. *Archives of pharmacal research*. 2009;32(5):767–72. Available at: <http://www.ncbi.nlm.nih.gov/pubmed/19471892>. Accessed July 18, 2014.
109. Yan Y-D, Sung JH, Kim KK, et al. Novel valsartan-loaded solid dispersion with enhanced bioavailability and no crystalline changes. *International journal of pharmaceutics*. 2012;422(1-2):202–10. Available at: <http://www.ncbi.nlm.nih.gov/pubmed/22085435>. Accessed July 18, 2014.
110. Kennedy M, Hu J, Gao P, et al. Enhanced bioavailability of a poorly soluble VR1 antagonist using an amorphous solid dispersion approach: a case study. *Molecular pharmaceutics*. 2008;5(6):981–993. Available at: <http://www.ncbi.nlm.nih.gov/pubmed/19434920>.
111. Shah N, Iyer RM, Mair H, et al. Improved Human Bioavailability of Vemurafenib, a Practically Insoluble Drug, Using an Amorphous Polymer-Stabilized Solid Dispersion Prepared by a Solvent-Controlled Coprecipitation. *Journal of pharmaceutical sciences*. 2013;102(3):967–981. Available at: <http://onlinelibrary.wiley.com/doi/10.1002/jps.23425/full>.
112. He H, Yang R, Tang X. In vitro and in vivo evaluation of fenofibrate solid dispersion prepared by hot-melt extrusion. *Drug development and industrial pharmacy*. 2010;36(6):681–7. Available at: <http://www.ncbi.nlm.nih.gov/pubmed/20136483>. Accessed July 17, 2014.
113. Onoue S, Kojo Y, Aoki Y, Kawabata Y, Yamauchi Y, Yamada S. Physicochemical and Pharmacokinetic Characterization of Amorphous Solid Dispersion of Tranilast with Enhanced Solubility in Gastric Fluid and Improved Oral Bioavailability. *Drug Metabolism and Pharmacokinetics*. 2012;27(4):379–387. Available

at: <http://jlc.jst.go.jp/JST.JSTAGE/dmpk/DMPK-11-RG-101?lang=en&from=CrossRef&type=abstract>. Accessed July 17, 2014.

114. Srinarong P, de Waard H, Frijlink HW, Hinrichs WLJ. Improved dissolution behavior of lipophilic drugs by solid dispersions: the production process as starting point for formulation considerations. *Expert opinion on drug delivery*. 2011;8(9):1121–40. Available at: <http://www.ncbi.nlm.nih.gov/pubmed/21722000>.

115. Paudel A, Worku ZA, Meeus J, Guns S, Van den Mooter G. Manufacturing of solid dispersions of poorly water soluble drugs by spray drying: formulation and process considerations. *International journal of pharmaceutics*. 2013;453(1):253–84. Available at: <http://www.ncbi.nlm.nih.gov/pubmed/22820134>. Accessed July 12, 2014.

116. Veiga MD, Bernad MJ, Escobar C. Thermal behaviour of drugs from binary and ternary systems. *International journal of pharmaceutics*. 1993;89:119–124. Available at: <http://www.sciencedirect.com/science/article/pii/037851739390112S#>.

117. Sheen P, Khetarpal VK, Cariola CM, Rowlings CE. Formulation studies of a poorly water-soluble drug in solid dispersions to improve bioavailability. *International journal of pharmaceutics*. 1995;118(2):221–227. Available at: <http://www.sciencedirect.com/science/article/pii/037851739400366D>.

118. Saers ES, Nystrijm C, Ald M. Physicochemical aspects of drug release. XVI. The effect of storage on drug dissolution from solid dispersions and the influence of cooling rate and incorporation of surfactant. *International journal of pharmaceutics*. 1993;90:105–118. Available at: <http://www.sciencedirect.com/science/article/pii/0378517393901478>.

119. Alden M, Tegenfeldt J, Sjokvist E. Structure of solid dispersions in the system polyethylene glycol-griseofulvin with additions of sodium dodecyl sulphate. *International journal of pharmaceutics*. 1992;83:47–52. Available at: <http://www.sciencedirect.com/science/article/pii/0378517382900060>.

120. Forster a, Hempenstall J, Tucker, Rades T. The potential of small-scale fusion experiments and the Gordon-Taylor equation to predict the suitability of drug/polymer blends for melt extrusion. *Drug development and industrial pharmacy*. 2001;27(6):549–60. Available at: <http://www.ncbi.nlm.nih.gov/pubmed/11548862>.

121. DiNunzio JC, Brough C, Miller D a, Williams RO, McGinity JW. Applications of KinetiSol dispersing for the production of plasticizer free amorphous solid dispersions. *European journal of pharmaceutical sciences : official journal of the European Federation for Pharmaceutical Sciences*. 2010;40(3):179–87. Available at: <http://www.ncbi.nlm.nih.gov/pubmed/20230894>. Accessed July 19, 2014.

122. Dinunzio JC, Brough C, Hughey JR, Miller D a, Williams RO, McGinity JW. Fusion production of solid dispersions containing a heat-sensitive active ingredient by hot melt extrusion and Kinetisol dispersing. *European journal of pharmaceutics and biopharmaceutics : official journal of Arbeitsgemeinschaft für Pharmazeutische Verfahrenstechnik e.V.* 2010;74(2):340–51. Available at: <http://www.ncbi.nlm.nih.gov/pubmed/19818402>. Accessed July 19, 2014.

123. Mahlin D, Ponnambalam S, Höckerfelt MH, Bergström C a S. Toward in silico prediction of glass-forming ability from molecular structure alone: a screening tool in early drug development. *Molecular pharmaceutics*. 2011;8(2):498–506. Available at: <http://www.ncbi.nlm.nih.gov/pubmed/21344945>.
124. Guns S, Dereymaker A, Kayaert P, Mathot V, Martens J a, Van den Mooter G. Comparison between hot-melt extrusion and spray-drying for manufacturing solid dispersions of the graft copolymer of ethylene glycol and vinylalcohol. *Pharmaceutical research*. 2011;28(3):673–82. Available at: <http://www.ncbi.nlm.nih.gov/pubmed/21104299>. Accessed July 12, 2014.
125. Kim J-S, Kim M-S, Park HJ, Jin S-J, Lee S, Hwang S-J. Physicochemical properties and oral bioavailability of amorphous atorvastatin hemi-calcium using spray-drying and SAS process. *International journal of pharmaceutics*. 2008;359(1-2):211–9. Available at: <http://www.ncbi.nlm.nih.gov/pubmed/18501538>. Accessed July 17, 2014.
126. Chokshi R, Zia H. Hot-Melt Extrusion Technique : A Review. *Iranian journal of pharmaceutical research*. 2004;3:3–16. Available at: https://www.ijpr.sbmu.ac.ir/pdf_290_799880c70748d24fb06fec28351e1577.
127. Breitenbach J. Melt extrusion: from process to drug delivery technology. *European journal of pharmaceutics and biopharmaceutics : official journal of Arbeitsgemeinschaft für Pharmazeutische Verfahrenstechnik e.V.* 2002;54(2):107–17. Available at: <http://www.ncbi.nlm.nih.gov/pubmed/12191680>.
128. Abdelwahed W, Degobert G, Stainmesse S, Fessi H. Freeze-drying of nanoparticles: formulation, process and storage considerations. *Advanced drug delivery reviews*. 2006;58(15):1688–713. Available at: <http://www.ncbi.nlm.nih.gov/pubmed/17118485>. Accessed July 10, 2014.
129. Yasuji T, Takeuchi H, Kawashima Y. Particle design of poorly water-soluble drug substances using supercritical fluid technologies. *Advanced drug delivery reviews*. 2008;60(3):388–98. Available at: <http://www.ncbi.nlm.nih.gov/pubmed/18068261>. Accessed July 17, 2014.